Cancer Biology

ScRNA-seq of Diverse Pheochromocytoma Patients Reveals Distinct Microenvironment Characteristics and Supports an Informative Molecular Classification System

Reviewed Preprint

Published from the original preprint after peer review and assessment by eLife.

About eLife's process

Reviewed preprint posted
September 12, 2023 (this version)

Posted to bioRxiv
March 27, 2023

Sent for peer review
March 26, 2023

Sen Qin, Yawei Xu, Shimiao Yu, Wencong Han, Shiheng Fan, Wenxiang Ai, Kenan Zhang, Yizhou Wang, Xuehong Zhou, Qi Shen, Kan Gong, Luyang Sun, Zheng Zhang

Department of Biochemistry and Molecular Biology, School of Basic Medical Sciences, Department of Urology, Peking University First Hospital, Peking University Health Science Center, Beijing 100191, China • Shenzhen Institute of Ladder for Cancer Research, Shenzhen 518020, China

Abstract

Pheochromocytomas (PCCs) are rare neuroendocrine tumors that originate from chromaffin cells in the adrenal gland. However, the cellular molecular characteristics and immune microenvironment of PCCs are incompletely understood. Here, we performed single-cell RNA sequencing (scRNA-seq) on 16 tissues from 4 sporadic unclassified PCC patients and 1 hereditary PCC patient with Von Hippel-Lindau (VHL) syndrome. We found that intra-tumoral heterogeneity was less extensive than the inter-individual heterogeneity of PCCs, a finding inconsistent with the widely-used PASS evaluation system. We further divided the unclassified PCC patients into two types, metabolism-type (marked by NDUFA4L2 and COX4I2) and kinase-type (marked by RET and PNMT), validated by immunohistochemical staining. Trajectory analysis of tumor evolution revealed that metabolism-type PCC cells display phenotype of consistently active metabolism and increased malignant potential, while kinase-type PCC cells showed decreased epinephrine synthesis and neuron-like phenotypes. Cellular communication analysis showed activation of the annexin pathway and a strong inflammation reaction in metabolism-type PCCs and activation of FGF signaling in the kinase-type PCC. Although multispectral immunofluorescence staining showed a lack of $CD8^+$ T cell infiltration in both metabolism-type and kinase-type PCCs, only the kinase-type PCC exhibited downregulation of *HLA-I* molecules that possibly regulated by *RET*, suggesting the potential of combined therapy with kinase inhibitors and immunotherapy for kinase-type PCCs; in contrast, the application of immunotherapy to metabolism-type PCCs (with antigen presentation ability) is likely unsuitable. Our study presents a single-cell transcriptomics-based molecular classification and microenvironment characterization of PCCs, providing clues for potential therapeutic strategies to treat PCCs.

eLife

eLife assessment

This study presents a **valuable** finding for the treatment of PCCs by sequencing 16 tumor specimens from five patients with pheochromocytomas by single-cell transcriptomics and proposing a new molecular classification criterion based on the sequencing results and characterization of tumor microenvironmental features. The evidence supporting the claims of the authors is **solid**, although the inclusion of more patient samples would strengthen the study's conclusions. The work will be of interest to clinicians or medical biologists working on rare pheochromocytomas (PCCs).

Introduction

Pheochromocytomas (PCCs) are rare neuroendocrine tumors that originate from chromaffin cells in the adrenal gland (Fishbein *et al*, 2017; Toledo *et al*, 2017). PCCs have been shown to display a remarkable diversity of driver alterations, including germline and somatic mutations as well as somatic fusion genes (Favier *et al*, 2015; Fishbein *et al*., 2017; Pillai *et al*, 2017). This diversity is reflected in the current molecular taxonomy of PCCs The Cancer Genome Atlas (TCGA), including for example the pseudo-hypoxic type (germline mutations in *SDHx*, *FH*, and *VHL*, etc.), the kinase-signaling type (germline or somatic mutations in *RET*, *NF1*, *TMEM127*, *MAX*, and *HRAS*, etc.), and the Wnt-signaling type (somatic mutations in *CSDE1* and somatic gene fusions affecting *MAML3*) (Crona *et al*, 2017). However, 50~60% of PCCs fail to be classified using this system (Lenders *et al*, 2014).

As understanding of PCC clinicopathological and immunophenotypic characteristics has deepened, the former concept of 'benign or malignant PCC' has been abandoned; since 2017, all PCCs are regarded as malignant tumors with metastatic potential according to the WHO pathological classification (Lam, 2017). There is no single histo-morphological feature indicating the malignant potential of PCCs; a number of multifactorial systems have been proposed (Kulkarni *et al*, 2016). A cytomorphometric study reported that extra-adrenal location, coarse nodularity, confluent necrosis, and the absence of hyaline globules are associated with malignant behavior (Lewis, 1971). Several scoring systems that for example consider vascular invasion, tumor size, diffuse growth, and mitotic activity have been used for risk assessment of malignant behavior of PCCs (Sherwin, 1959; Sisson *et al*, 1984; Symington & Goodall, 1953). A scoring system—the Pheochromocytoma of the Adrenal gland Scaled Score (PASS)—is weighted for histologic features and has been used to separate tumors with a potential for a biologically aggressive behavior (PASS > or = 4) from tumors with benign lesion (PASS < 4) (Thompson, 2002). However, there have been conflicting reports regarding the utility of the PASS scoring system in correctly predicting PCC malignancy (Agarwal *et al*, 2010; Strong *et al*, 2008; Wu *et al*, 2009).

Immune checkpoint inhibitors (ICIs) have achieved remarkable results in a variety of solid tumors in recent years (Brahmer *et al*, 2012; Herbst *et al*, 2014; Ribas & Wolchok, 2018). Currently, there are only 2 clinical trials investigating the efficacy of ICIs for the treatment of metastatic PCCs: one is still in the recruitment stage, and the other showed 43% non-progression rate (NPR) and 0% overall response rate (ORR) in 7 PCC patients (Dai *et al*, 2020; Naing *et al*, 2020). The composition of immune cells in the tumor immune microenvironment is an essential indicator for predicting likely responses to immunotherapy, and serves as the basis of immunotherapy (Joyce & Fearon, 2015; Schumacher & Schreiber, 2015). However, there are no studies reporting the composition of immune cells in PCCs. The few published studies investigating the immune microenvironment of PCCs have been limited to the expression of PD-L1 at the histological level

and to assessment of the tumor mutation burden (TMB) at the genomic level, and these results only seem to suggest that PCCs are immune-cold (Bratslavsky *et al*, 2019; Guo *et al*, 2019; Pinato *et al*, 2017). Therefore, deepening understanding of the immune cell composition in the tumor immune microenvironment should greatly aid in the effective application of immunotherapies to treat PCCs (Uher *et al*, 2021).

In the present study, we performed single-cell RNA sequencing (scRNA-seq) analysis of 11 tumor tissues and 5 adjacent tissues from 4 sporadic PCC patients with unclassified mutations and 1 hereditary PCC patient with Von Hippel-Lindau (VHL) syndrome caused by germline mutation in *VHL*. We found less intra-tumoral heterogeneity than inter-individual heterogeneity of PCCs, which is inconsistent with the PASS score prediction, thus highlighting limitations of the PASS scoring system. For the unclassified PCCs, we distinguished metabolism-type and kinase-type PCCs based on copy number variants (CNVs) and gene expression profile data. These two PCC types also displayed distinct characteristics of tumor evolution and cell-cell communication. Although multispectral immunofluorescence staining showed a lack of $CD8^+$ T cell infiltration in both metabolism-type and kinase-type PCCs, only the kinase-type PCC exhibited downregulation of *HLA-I* molecules that possibly regulated by *RET*, suggesting the potential of combined therapy with kinase inhibitors and immunotherapy for kinase-type PCCs, whereas the application of immunotherapy to metabolism-type PCCs (with antigen presentation ability) is likely unsuitable. Our study presents a single-cell transcriptomics-based molecular classification and microenvironment characterization of PCCs and provides clues for potential therapeutic strategies to treat PCCs.

Results

A Landscape View of Cell Composition in PCCs

To characterize the molecular correlates of unclassified PCCs based on known prominent driver alterations, we performed single-cell RNA sequencing (scRNA-seq) on 16 collected specimens from 5 PCC patients (P1-P5). Four of these patients (P1-P4) suffered from sporadic PCCs: whole exome sequencing (WES) of these tumor tissues detected somatic mutations as compared with their adjacent tissues, including in *JAK2*, *ARHGEF39*, *KMT2D*, and *MST1* (Supplemental Table S1); note that none of these fit into the three previously molecularly defined groups in the TCGA molecular taxonomy (Crona *et al*., 2017). The cohort also included 1 hereditary PCC patient (P5) with Type 2 Von Hippel-Lindau (VHL) syndrome, with a germline missense mutation in *VHL* (Supplemental Table S1).

We collected 1 resected tumor specimen from P1 (P1_T1), 3 specimens from distinct intra-tumoral sites from P2 (P2_T1, P2_T2, and P2_T3) and P5 (P5_T1, P5_T2, and P5_T3), as well as 2 specimens from distinct intra-tumoral sites from P3 (P3_T1 and P3_T2), and P4 (P4_T1 and P4_T2). To enable comparisons, one adrenal tissue specimen adjacent to the tumor was collected from each patient (P1_A, P2_A, P3_A, P4_A, and P5_A) (**Fig. 1A**). Tumor cell morphology was observed with microscopy of hematoxylin-eosin stained tumor tissues (Fig. S1), and immunocytochemistry staining results showed strong expression of Chromogranin A (CGA) in all tumor tissues, validating that the collected samples were PCC tumor specimens (Fig. S1). The histological features of samples were evaluated with the PASS scoring system for predicting the malignant potential of PCC patients. The PASS scores ranged from 2 to 9, showing obvious heterogeneity among the examined intra-tumoral sites and inter-individual comparisons for the 5 PCC patients (Supplemental Table S2).

The specimens were digested into single cell suspensions, and 3'-scRNA-seq (Chromium Single Cell 3' v3 Libraries) analysis was performed on each sample. After quality control filtering to remove cells with low gene detection and high mitochondrial gene coverage, we retained 133,894

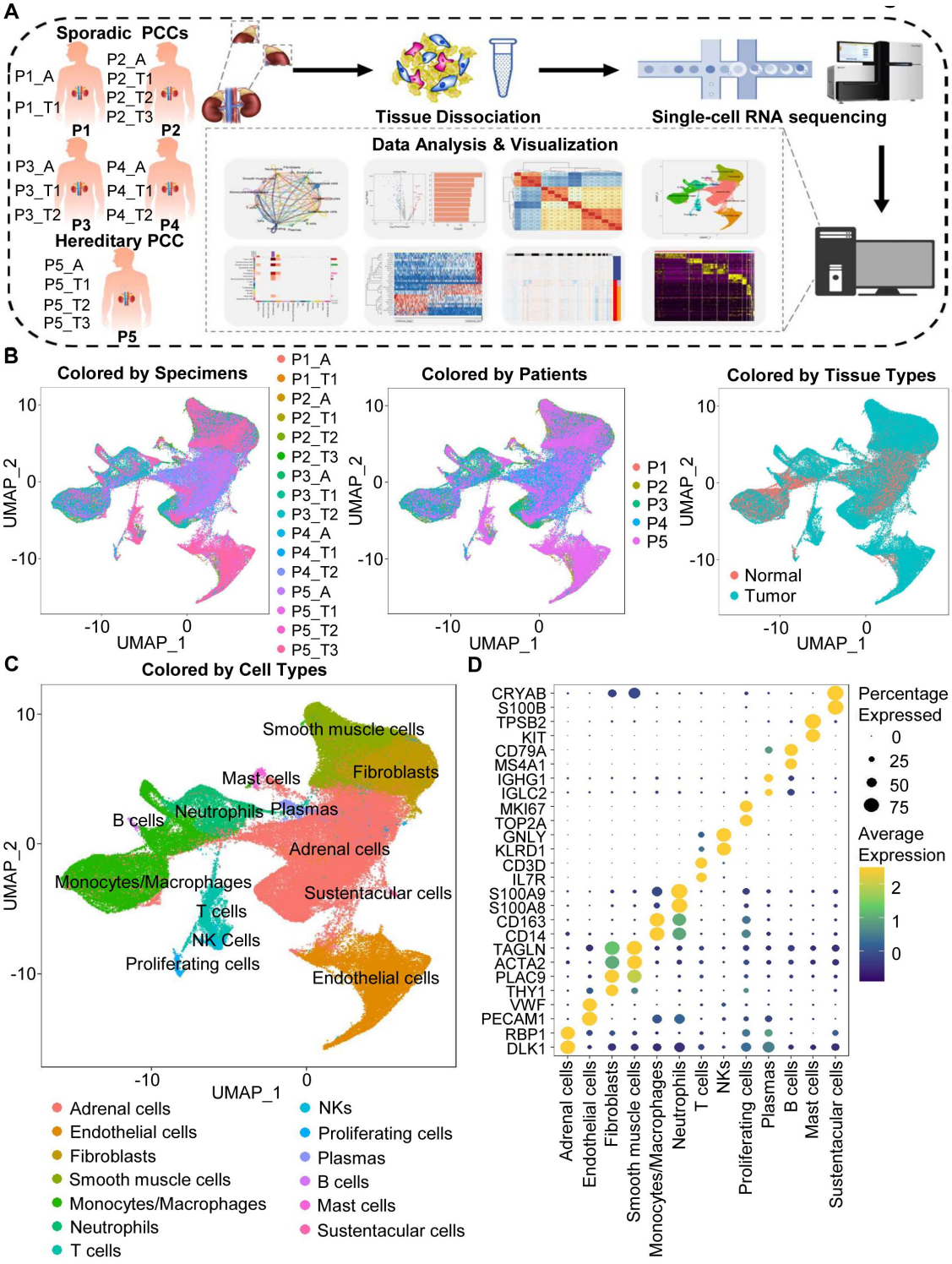

Figure 1.

Integration Analysis across 5 PCC Patients Revealing the Cell Composition of the PCC Microenvironment.

(A) Schematic of the experimental pipeline. 11 tumor specimens and 5 adjacent specimens were isolated from 5 PCC patients, dissociated into single-cell suspensions, and analyzed using 10x Genomics Chromium droplet scRNA-seq. (B) UMAP plots displaying 133,894 cells isolated from 16 specimens collected from 5 PCC patients. (B) UMAP plots of cells colored by specimens, patients, and tissue types. (C) UMAP plot showing 13 main cell types from all specimens. (D) Dot plot of representative marker genes for each cell type. The color scale represents the average marker gene expression level; dot size represents the percentage of cells expressing a given marker gene.

individual cells (Fig. S2A-S2C). SCTansformed normalization and principal component analysis (PCA) of the Seurat suite(Butler *et al*, 2018; Satija *et al*, 2015; Stuart *et al*, 2019) were then employed for unsupervised dimensionality reduction prior to clustering. Uniform Manifold Approximation and Projection (UMAP) was used for visualizing the distinct specimens, patients, and tissue types (**Fig. 1B** and **1C**).

We classified the 67 detected clusters into 13 cell types according to their expression profiles for recognized marker genes and Spearman correlation analysis between clusters: the classified cell types included adrenal cells (marked by *DLK1* and *RBP1*), endothelial cells (marked by *PECAM1* and *VWF*), fibroblasts (marked by *THY1* and *PLAC9*), smooth muscle cells (marked by *ACTA2* and *TAGLN*), monocytes/macrophages (marked by *CD14* and *CD163*), neutrophils (marked by *S100A8* and *S100A9*), T cells (marked by *IL7R* and *CD3D*), natural killer cells (NKs, marked by *KLRD1* and *GNLY*), proliferating cells (marked by *TOP2A* and *MKI67*), plasma cells (marked by *IGLC2* and *IGHG1*), B cells (marked by *MS4A1* and *CD79A*), mast cells (marked by *KIT* and *TPSB2*), and sustentacular cells (marked by *S100B* and *CRYAB*) (**Fig. 1C** and **1D**, Fig. S2D and S2E). Thus, our clustering and cell type annotation analysis identified diverse adrenal cells, stromal cells, and immune cells within the PCC microenvironment.

The PASS Score does not Informatively Reflect Heterogeneity as Inferred from the scRNA-seq Data

In light of the remarkable diversity of drivers including germline and somatic mutations reported among PCCs (Crona *et al*., 2017), we investigated PCC heterogeneity at the inter-individual and intra-tumoral levels based on the single-cell transcriptional profiles. A Spearman correlation analysis based on average gene expression in each specimen showed that the intra-tumoral heterogeneity was less than inter-individual heterogeneity (**Fig. 2A**), inconsistent with the PASS score prediction. We further analyzed the cell type composition in each specimen and found similar fractions of cell types between the collected intra-tumoral sites despite different PASS scores (**Fig. 2B**), indicating relatively small intra-tumoral differences in both gene expression and cell type composition.

The inter-individual correlation analysis indicated that P4 showed low correlation with the other three sporadic PCCs patients (P1-P3) (**Fig. 2C**), and further analysis of cell type fractions showed a significantly elevated proportion of adrenal cells (77%) in P4; the adrenal cells comprised between 16–36% of the total cells in the P1-P3 specimens (**Fig. 2D**). P4 also had an obviously distinct distribution of stromal cells *vs* immune cells (9% stromal cells and 14% immune cells) as compared to P1-P3 (28-62% stromal cells and 22-43% immune cells) (**Fig. 2D**). Consistent with the reported vascular endothelial hyperplasia phenotype in VHL syndrome (Vortmeyer *et al*, 2013), it was unsurprising that we observed poor correlation between the sporadic patients (P1-P4) and the VHL patient (P5), reflecting a higher proportion of endothelial cells in P5 (35%) as compared to P1-P4 (3-10%) (**Fig. 2C** and **2D**).

Based on these observations, we proposed that there was a certain degree of limitation in the PASS scoring system that is based on the histologic observation of tumor tissues, which is consistent with the report that some patients with a low degree of malignancy based on the PASS scoring system exhibit invasion or metastasis (Agarwal *et al*., 2010; de Wailly *et al*, 2012; Wu *et al*., 2009), and the incorporation of PASS scoring system with gene expression profile might facilitate further understanding of PCC pathobiology and/or aid in the clinical evaluation of PCC.

Identification of Tumor Clusters through CNV analysis

To further characterize malignant chromaffin cells, we collected adrenal cells, which theoretically include adrenocortical cells and chromaffin cells (Yates *et al*, 2013). The copy number karyotyping of aneuploid tumors (CopyKAT) algorithm (Gao *et al*, 2021) was applied, which estimates genomic copy number variants (CNVs) from scRNA-seq data by employing an integrative

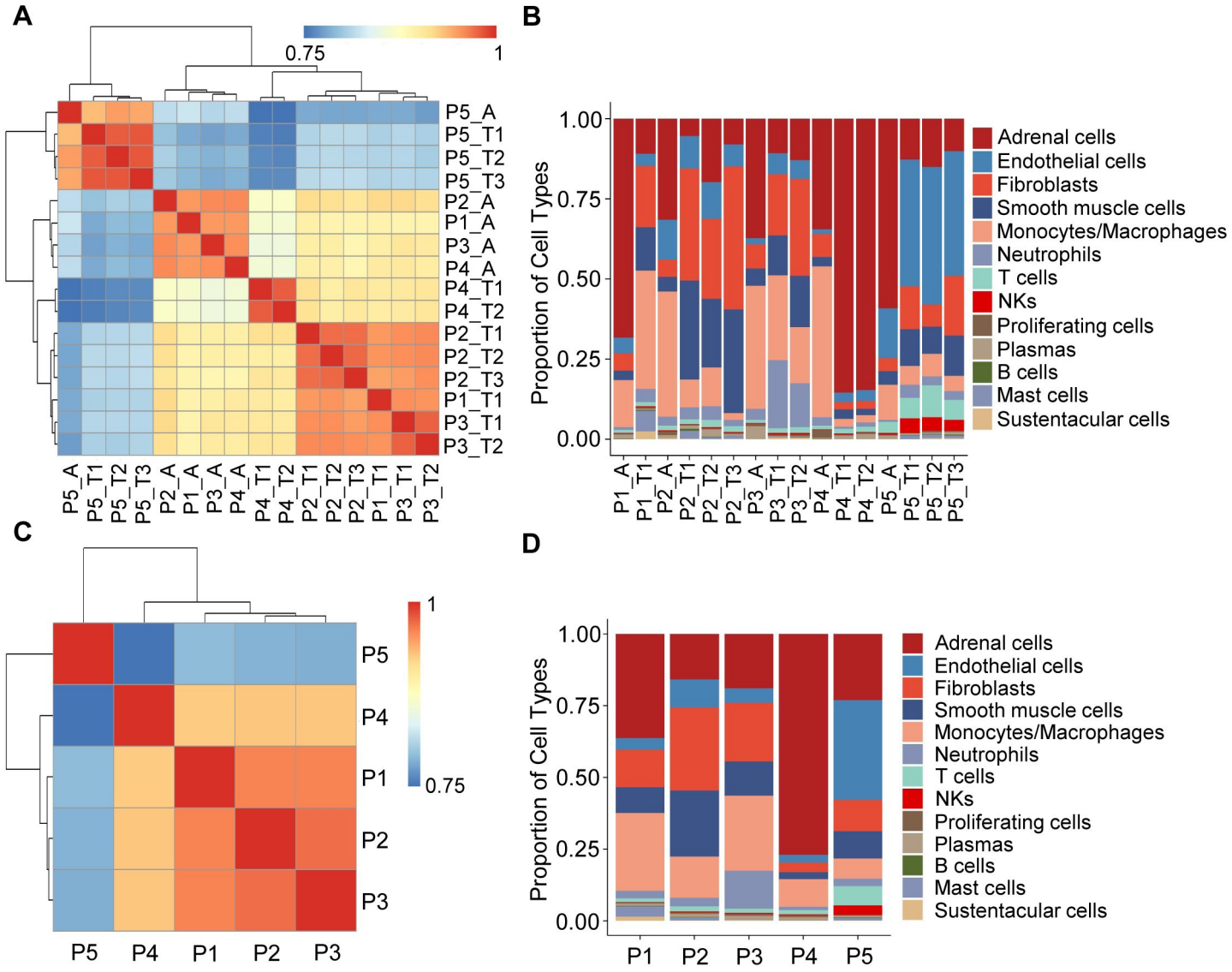

Figure 2.

Correlation Analysis Reveals Less intra-tumoral Heterogeneity than inter-individual Heterogeneity.

(A) Heatmap plotting the correlation coefficient among 16 specimens. The color keys from blue to red indicate the correlation coefficient from low to high. (B) Bar plot showing the percentage of cell types in 16 specimens. (C) Heatmap of the correlation coefficient among 5 PCC patients. The color keys from blue to red indicate the correlation coefficient from low to high. (D) Bar plot depicting the frequency distribution of cell types in 5 PCC patients.

Bayesian segmentation approach to distinguish malignant chromaffin cells from normal cells. Our analysis identified two clusters among adrenal cells (normal cells and tumor cells), with tumor cells showing extensive chromosomal amplification and/or deletion (**Fig. 3A**). Consistently, the inferred aneuploid tumor cells highly expressed *Chromogranin B* (*CHGB*), which is a marker of malignant chromaffin cells (Wiedenmann *et al*, 1988; Winkler & Fischer-Colbrie, 1992) (**Fig. 3B** and **3C**). The inferred diploid normal cells expressing high levels of *CYP17A1* and *HSD3B2* were defined as adrenocortical cells (Kubota-Nakayama *et al*, 2016), while the inferred diploid normal cells showing low *CHGB* expression were defined as normal chromaffin cells (**Fig. 3B** and **3C**). We also found a cluster of inferred diploid normal cells with high expression of *VWF* (a marker for vascular endothelial cells) in the VHL patient (P5) (**Fig. 3B** and **3C**).

We noticed two CNV patterns among the inferred aneuploid tumor cells, with the distinction evident in chromosomes 3, 11, and 17 (**Fig. 3A**). These CNV profiles were reflected in distinct tumor clusters (tumor cluster A and B) through CopyKAT prediction (**Fig. 3D**). We observed that cells in inferred tumor cluster A exhibited high expression of *NDUFA4L2* and *COX4I2*, while cells in inferred tumor cluster B expressed high levels of *PNMT* and *RET* (**Fig. 3D** and **3E**), suggesting the different gene expression between tumor cluster A and B. PNMT is known as an enzyme that catalyzes the conversion of norepinephrine to epinephrine and that RET is a member of the receptor tyrosine kinase family, while NDUFA4L2 and COX4I2 respectively function in the oxidative phosphorylation and glycolysis pathways (Drilon *et al*, 2018; Mahmoodi *et al*, 2020; Sinkler *et al*, 2017). Taken together, we distinguished malignant chromaffin cells from adrenal cells through CNV analysis and found two clusters of malignant chromaffin cells with different single-cell copy number profiles.

Definition of Metabolism-type and Kinase-type tumors among unclassified PCCs

To explore the gene expression profile between tumor cluster A and B, we then used the FindAllMarkers function of the Seurat suite (Butler *et al*., 2018; Satija *et al*., 2015; Stuart *et al*., 2019) to identify differentially expressed genes (DEGs) of these tumor clusters (**Fig. 4A** and **4B**). A functional enrichment analysis based on gene ontology (GO) annotation was performed to further characterize the biological function of tumor clusters: the tumor cluster A DEGs showed functional enrichment for terms including generation of metabolites and energy, response to oxygen levels, response to hypoxia, and ATP metabolic process and some notably upregulated genes of tumor cluster A included known energy metabolism-related genes such as *NDUFA4L2*, *COX4I2*, *RGS4*, and *AQP1* (**Fig. 4C**). For tumor cluster B, the GO analysis showed enrichment for terms including cytoplasmic translation, neuron projection development, axon development, and cell growth, and there was obvious upregulation of *PNMT*, *RET*, and genes encoding other kinases known to function in proliferation, as well as genes that participate in the regulation of neuroendocrine functions (*e.g.*, *CALM1*, *PENK*, and *NPY*) (**Fig. 4D**).

Notably, immunocytochemistry staining of serial tumor sections showed strong accumulation of PNMT and RET in P4, while NDUFA4L2 and COX4I2 accumulation was characteristic for the P1-P3 and P5 sections, providing protein-level evidence to validate the differential trends detected from the scRNA-seq results (**Fig. 4E**). As a consequence, we propose a metabolism-type (P1-P3) and kinase-type (P4) classification for unclassified sporadic PCCs. Consistently, kinase-signaling PCCs by TCGA classification include germline and somatic mutations in *RET*, and are uniquely able to secrete epinephrine, owing to their high expression of *PNMT*; P5 could also be classified into the metabolism-type we defined, which is known to display reprogramming of cellular energy metabolism caused by *VHL* mutation and subsequent *HIF* dysregulation (Chappell *et al*, 2019). These results support that the previously unclassified PCCs can be classified as metabolism-type or kinase-type based on transcriptional programs, with these types partially corresponding to the pseudo-hypoxic type and kinase-signaling type of PCCs from the TCGA classification.

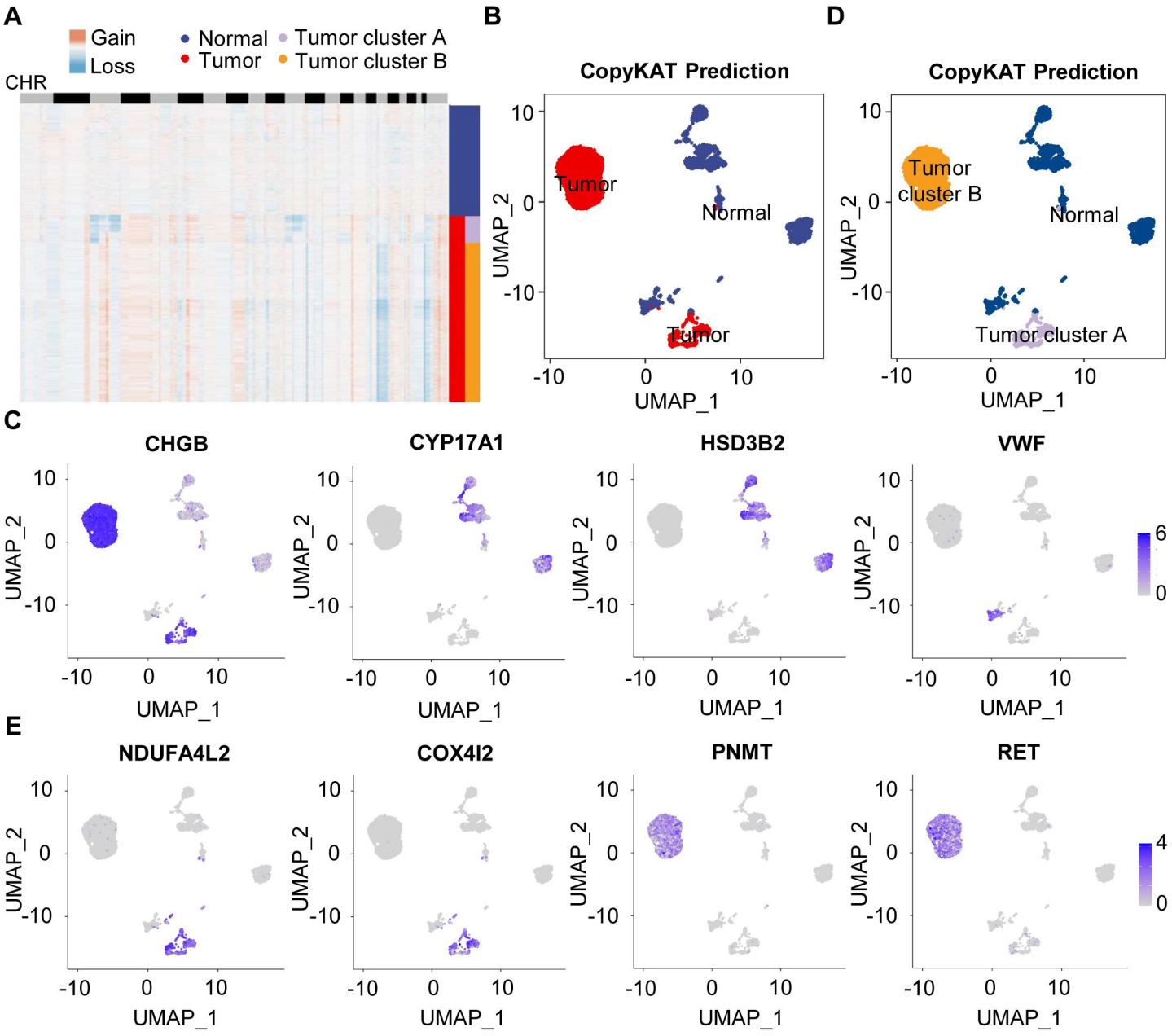

Figure 3.

Single-cell Copy Number Profiles in PCC Clusters Inferred by CopyKAT.

(A) Heatmap indicating the CNV patterns of inferred normal cells, tumor cells, tumor cluster A, and tumor cluster B. Blue, white, and red respectively indicate deletion from a chromosome, normal chromosome, and amplification on a chromosome. (B) UMAP plot of the inferred normal cells (blue) and tumor cells (red) identified by CopyKAT. (C) Feature plots showing the marker gene expression levels in inferred normal cells and tumor cells. (D) UMAP plot depicting the inferred normal cells (blue), tumor cluster A (purple), and tumor cluster B (orange) identified by CopyKAT. (E) Feature plots displaying the marker gene expression levels in inferred tumor cluster A and B.

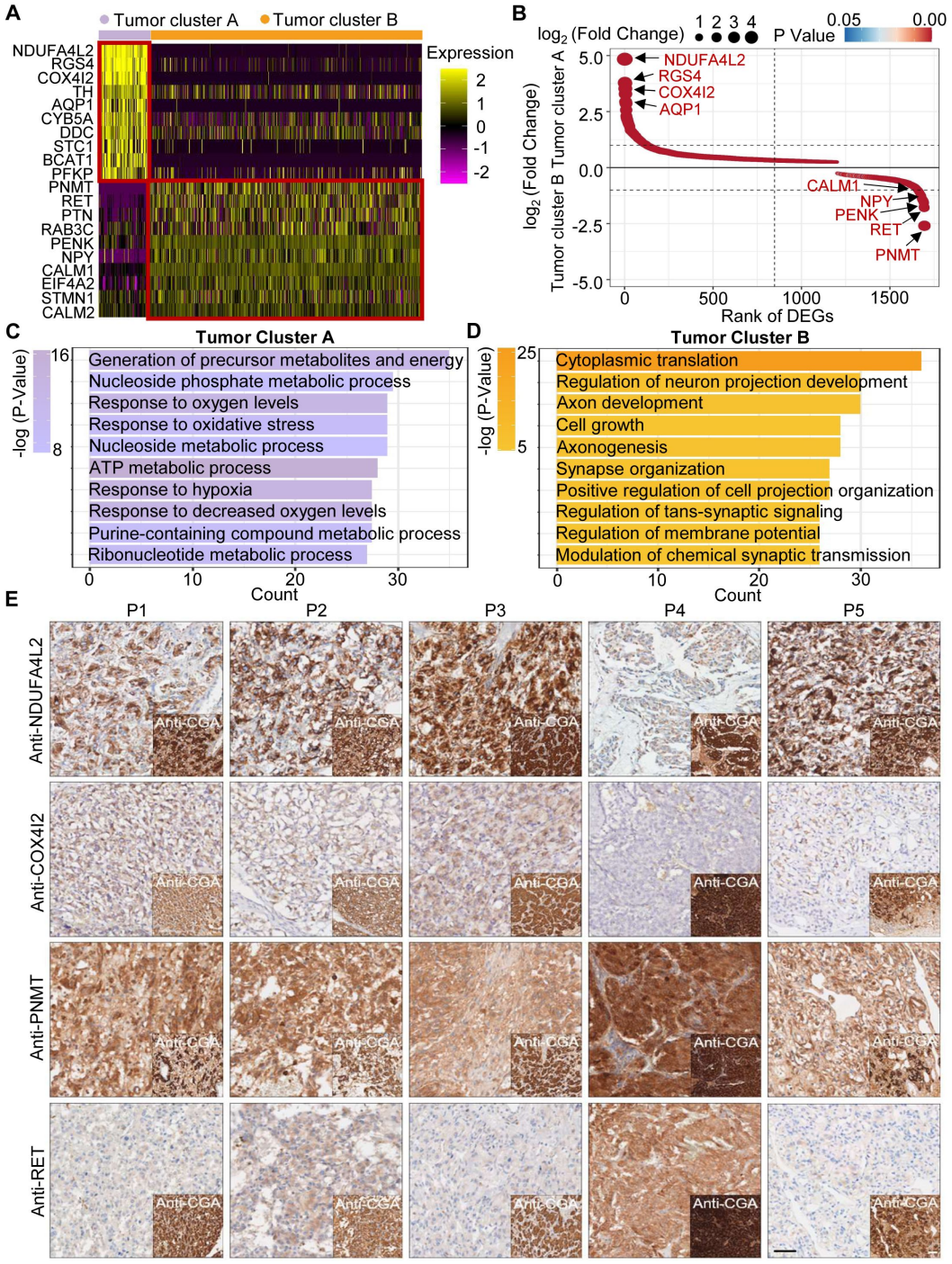

Figure 4.

PCC Patients were Classified into Metabolism-type and Kinase-type.

(A) Heatmap plotting the scaled expression patterns of major marker genes in each tumor cluster. The color keys from pink to yellow indicate relative expression levels from low to high. (B) Dot plot depicting up-regulated genes of tumor cluster A (top) and tumor cluster B (bottom). The x-axis specifies the rank of DEGs and the y-axis specifies the natural logarithm of the FC. Dotted vertical and horizontal lines reflect the filtering criteria. Dot size represents the natural logarithm of the FC of genes. The color keys from blue to red indicate the P-value from high to low. (C, D) GO enrichment analysis of the up-regulated genes in tumor cluster A (C) and tumor cluster B (D) indicating the top altered 10 terms in the biological process of gene ontology. The x-axis specifies the number of genes enriched in the pathways. The color keys from shallow to deep indicate the P-value from high to low. (E) Immunohistochemistry staining of CGA, NDUFA4L2, COX4I2, PNMT, and RET markers in formalin-fixed paraffin-embedded PCC tissue sections matched to scRNA-seq specimens. Scale bar, 100 μm.

Trajectory Analysis Reveals Subclonal Dynamics of PCC Types

We next examined tumor subclonal evolution patterns for the metabolism-type and kinase-type PCCs, by applying the Dynverse algorithm to order cells along a pseudotime trajectory (Saelens *et al*, 2019). We first clustered metabolism-type PCC cells into 2 subclusters based on DEGs and found similar proportions of tumor subcluster 1 and 2 at both the early stage and late stage of tumor evolution (**Fig. 5A** and **5B**). Late up-regulated genes include *S100A4* and *TAGLN* that promote epithelial-mesenchymal transition and cell invasion, which highly expressed in subcluster 2 (**Fig. 5C**), suggesting the higher malignant potential of subcluster 2 as compared with subcluster 1. Metabolism-related genes such as *NDUFA4L2*, *ATP5MG*, *NDUFB4*, and *COX17* were highly expressed at early stage, while *SOD3* and *COX7A1* were up-regulated at the late stage (**Fig. 5C**), revealing the consistently active metabolism phenotype of metabolism-type PCCs cells. We also found the high expression of tumor suppressor gene *SPINT2* at early stage and subsequent up-regulation of the oncogene *JUNB* (**Fig. 5C**), revealing an increase of malignant potential over the tumor evolution of metabolism-type PCCs. In short, these results indicate that cells from metabolism-type PCCs display phenotype of consistently active metabolism and increasingly malignant potential.

We then clustered kinase-type PCC cells into 2 subclusters and found that the major clone has been changed from subcluster 1 to 2 along the trajectory (**Fig. 5D** and **5E**). Further analysis of DEGs in the pseudotime trajectory showed early high expression of *CALM1* and *CALM2* in the subcluster 1, and late up-regulation of *RET* in the subcluster 2 (**Fig. 5F**), suggesting the persistent dysregulation of kinase signals over tumor evolution. We also noticed the early expression of *PNMT*, while neuron-specific genes such as *MAP2*, *MAP1B*, *L1CAM*, and *CNTN1* were up-regulated later in the pseudotime trajectory (**Fig. 5F**), suggesting the decrease of epinephrine synthesis and the appearance of neuron-like phenotypes during tumor evolution, consistent with previously reported neuron-like phenotypes in PCC cells with high expression of RET (Califano *et al*, 1995; Powers *et al*, 2003; Powers *et al*, 2009). Taken together, these analyses have revealed the transcriptional clonal dynamics of metabolic-type and kinase-type PCCs.

Cellular Communication Analysis to Further Characterize the Tumor Microenvironment

Having characterized differences in the cell type composition, gene expression, and clonal evolution between metabolism-type and kinase-type PCCs, we subsequently expanded our investigation to cell-cell communication occurring within the distinct tumor microenvironments of these two types of PCCs. We adopted CellChat tool to quantitively analyze intercellular communication networks (Jin *et al*, 2021). We observed the activation of the annexin signaling pathway in metabolism-type PCCs (**Fig. 6A**). Further analysis of participated ligand-receptors showed major participation of *ANXA1-FPR1* pair in the annexin signaling pathway (**Fig. 6B**), and high co-expression of *ANXA1* and *FPR1* in neutrophils and monocytes/macrophages (**Fig. 6C**). It has been reported that the annexin signaling pathway is known to be activated under a strong inflammatory reaction (Gastardelo *et al*, 2014; Gavins *et al*, 2003; Gerke & Moss, 2002; Hayhoe *et al*, 2006). Combined with our findings of a higher proportion of neutrophils and monocytes/macrophages in metabolism-type as compared with kinase-type (**Fig. 2D**), we speculate that metabolism-type PCCs may display elevated inflammatory responses. We then performed Gene Set Enrichment Analysis (GSEA) on metabolism-type and kinase-type PCCs by using hallmark gene sets in the MSigDB databases (Liberzon *et al*, 2011). As expected, the inflammatory response signaling pathway showed enrichment in metabolism-type PCCs as compared with that in kinase-type PCC (**Fig. 6D**). Taken together, metabolism-type PCCs exhibited a strong inflammatory reaction and the activation of annexin signaling pathway.

Considering the heterogeneity in cell type composition between sporadic and VHL patients in metabolism-type, we further analyzed cellular interactions in the VHL patient. We noticed the activation of VEGF signaling pathway in P5 (**Fig. 6E**), and major contribution of *PLGF-VEGFR1*,

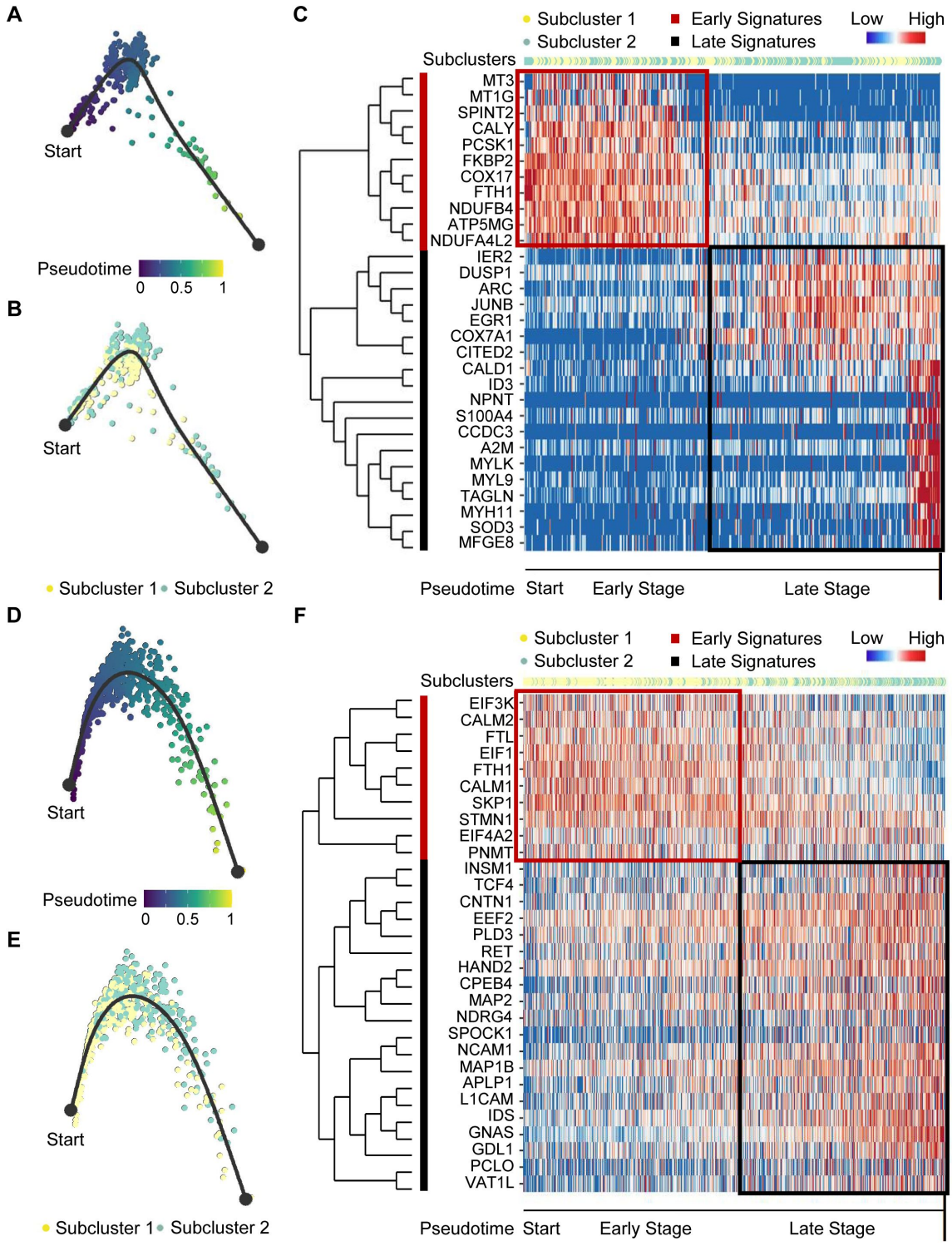

Figure 5.

Pseudotime Analysis of PCC Tumor Evolution by Dynverse.

(A, B) Pseudotime trajectory of metabolism-type PCC cells colored by pseudotime (A) and tumor subclusters (B). (C) Pseudotime heatmap plotting the expression levels of genes across the transition from beginning (left) to end (right). The color keys from blue to red indicate the gene expression levels from low to high. (D, E) Pseudotime trajectory of kinase-type PCC cells colored by pseudotime (D) and tumor subclusters (E). (F) Pseudotime heatmap showing the expression levels of genes across the transition from beginning (left) to end (right). The color keys from blue to red indicate the gene expression levels from low to high.

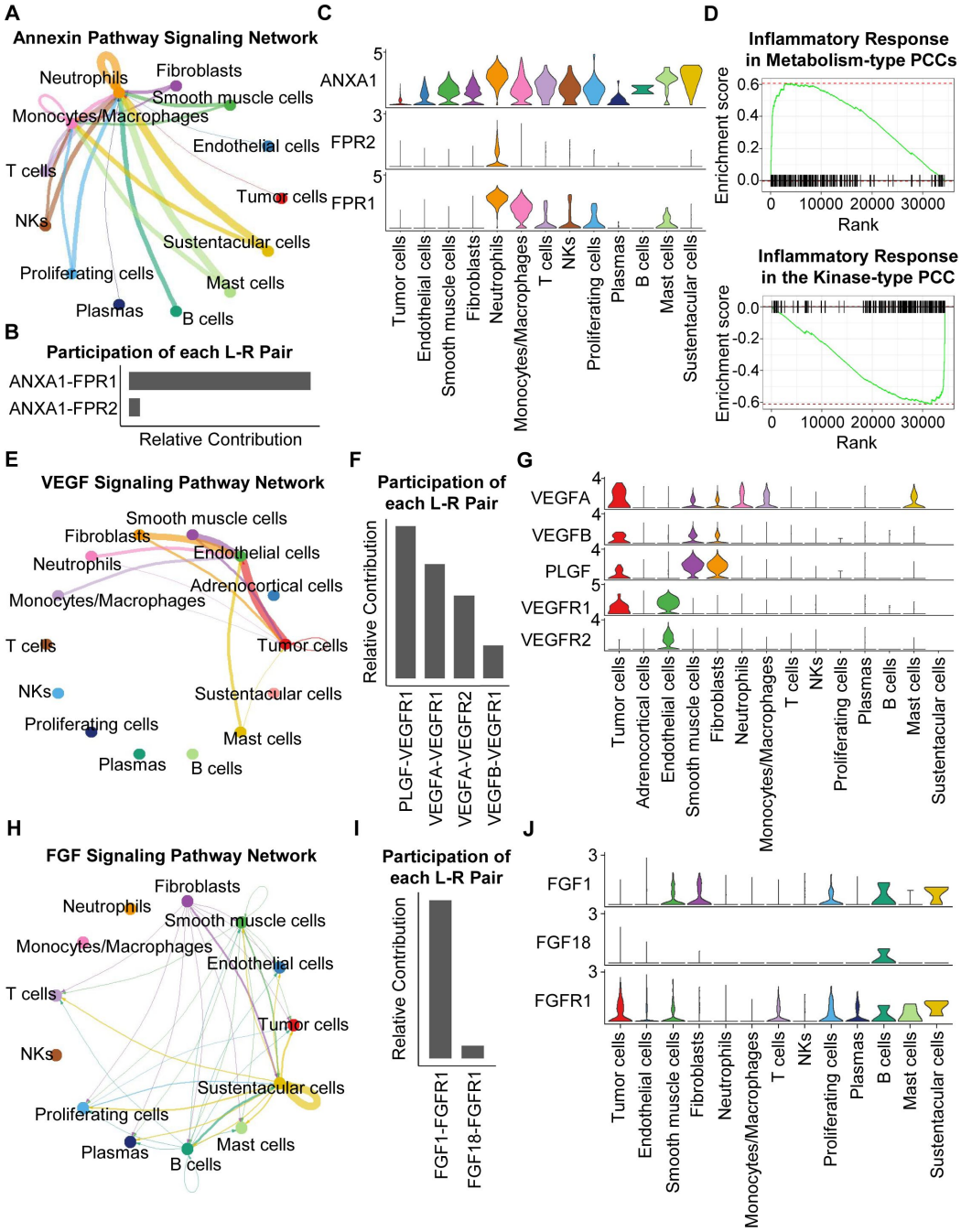

Figure 6.

CellChat Analysis Reveals Cell-cell Communication Patterns in PCC Types.

(A) Circle plot showing an inferred annexin signaling pathway network in the metabolism-type PCC microenvironment. The edges connecting the circles represent the communication probability between any two kinds of cell types. The color of the edge denotes directionality (i.e., senders *vs* receivers). (B) Bar graph plotting the quantification of the relative contributions of individual ligand-receptor pairs to the overall annexin signaling pathway. (C) Violin plot of the expression distribution of *ANXA1*, *FPR1*, and *FPR2* in main cell types of the metabolism-type PCC microenvironment. (D) GSEA enrichment plots of the inflammatory response signaling of metabolism-type patients (left) and the kinase-type patient (right). (E) Circle plot depicting an inferred VEGF signaling pathway. (F) Bar graph displaying the quantification of the relative contributions of individual ligand-receptor pairs to the overall VEGF communication network. (G) Violin plot plotting the expression distribution of *VEGFA*, *VEGFB*, *PLGF*, *VEGFR1*, and *VEGFR2* in main cell types of P5 PCC microenvironment. (H) Circle plot of an inferred FGF signaling pathway in the kinase-type PCC microenvironment. (I) Bar graph showing the quantification of the relative contributions of individual ligand-receptor pairs to the overall FGF signaling pathway. (J) Violin plot plotting the expression distribution of *FGF1*, *FGF18*, and *FGFR1* in main cell types of the kinase-type PCC microenvironment.

VEGFA-VEGFR1 and *VEGFA-VEGFR2* pairs to VEGF signaling pathway (**Fig. 6F**). Specifically, *VEGFA* and *VEGFR1* were highly expressed in tumor cells, *VEGFR1* and *VEGFR2* in endothelial cells, and *PLGF* in fibroblasts and smooth muscle cells, respectively (**Fig. 6G**), suggesting the crosstalk between tumor cells and fibroblasts or endothelial cells in tumor microenvironment through these ligand-receptor pairs, which mediated in the tumor angiogenesis and metastasis. The observed activation of VEGF pathway is consistent with the vascular endothelial hyperplasia caused by *VHL* mutation in VHL syndrome (Vortmeyer *et al*., 2013) and the elevated proportion of endothelial cells in this patient (**Fig. 2D**).

We subsequently analyzed the kinase-type PCC patient, and identified the activation of FGF signaling network (**Fig. 6H**) and major involvement of *FGF1-FGFR1* in the FGF pathway (**Fig. 6I**). The smooth muscle cells, fibroblasts, and B cells exhibited high expression of *FGF1*, while tumor cells, smooth muscle cells, T cells, and B cells highly expressed *FGFR1* (**Fig. 6J**). The analyses suggested the cell-cell communication among tumor cells, stroma cells, and immune cells through the *FGF1-FGFR1* pair, which regulated the tumor cell proliferation (Katoh, 2016). These results indicate that kinase-type PCCs may benefit from FGFR inhibitors, which have been shown to exert inhibitory effects on tumor proliferation (Liang *et al*, 2012). Together, we described the cellular communication networks in microenvironment of metabolism-type and kinase-type PCCs.

Immune Infiltration in the PCC Microenvironment Implies Patient Responses to Immunotherapy

We further analyzed the immune microenvironment of metabolism-type and kinase-type PCCs. Visualization of cellular communication showed apparent crosstalk between tumor cells and T cells in metabolism-type patients, while we were surprised to find a lack of apparent communication between tumor cells and T cells in the kinase-type patient (**Fig. 7A**). These results suggested that kinase-type PCC cells could evade immune surveillance of T cells and further indicated the immune escape potential of kinase-type PCCs. Considering leukocyte antigen-class I (HLA-I) surface level is known to represent the antigen-presenting abilities of tumor cells (Brea *et al*, 2016; Jhunjhunwala *et al*, 2021; Oh *et al*, 2019), we assessed *HLA-I* expression in PCC cells: the expression levels of *HLA-A*, *HLA-B*, and *HLA-C* were significantly lower in kinase-type PCC cells than in metabolism-type PCC cells (**Fig. 7B**). Consistently, immunohistochemistry staining of serial sections of tumor tissues showed lower expression of HLA-A in P4 as compared to that in other patients (**Fig. 7C**), providing a plausible explanation for the lack of interactions detected between tumor cells and T cells in the kinase-type PCC. In short, we discovered that the kinase-type PCC displayed an impaired *HLA-I* expression profile consistent with immune escape, while metabolism-type PCCs showed antigen-presenting abilities.

We additionally assessed the immune microenvironment of PCCs by subclustering immunotherapy-related immune cells and identified 8 clusters including central memory $CD4^+$ T cells ($CD4^+$ TCM, marked by *CD3D*, *CD3E*, *CD3G*, *CD4*, *CCR7*, and *IL7R*), effector memory $CD4^+$ T cells ($CD4^+$ TEM, marked by *CD3D*, *CD3E*, *CD3G*, *CD4*, and *IL7R*), $CD8^+$ T cells (marked by *CD3D*, *CD3E*, *CD3G*, *CD8A* and *CD8B*), natural killer T cells (NKTs, marked by *CD3E*, *KLRD1* and *GNLY*), natural killer cells (NKs, marked by *KLRD1* and *GNLY*), B cells (marked by *MS4A1* and *CD79A*), M1 macrophages (marked by *CD68*), and M2 macrophages (marked by *CD68* and *CD163*) (**Fig. 7D** and **7E**). Further analysis of immune cell type composition in metabolism-type and kinase-type PCCs showed an increase in the proportion of $CD4^+$ T cells, $CD8^+$ T cells, and M1 macrophages in tumor tissues as compared with that in adjacent tissues, while the proportion of M2 macrophages in adjacent tissues decreased as compared with that in tumor tissues (**Fig. 7F**).

The proportion and location of infiltrating immune cells in tumor tissues have been shown to be informative regarding responsivity to immunotherapy (Sade-Feldman *et al*, 2018; Stanton & Disis, 2016). In particular, the $CD8^+$ T cells play an essential role in anti-tumor immunity; these cells can recognize tumor antigens displayed on the surface of tumor cells by HLA-I molecules

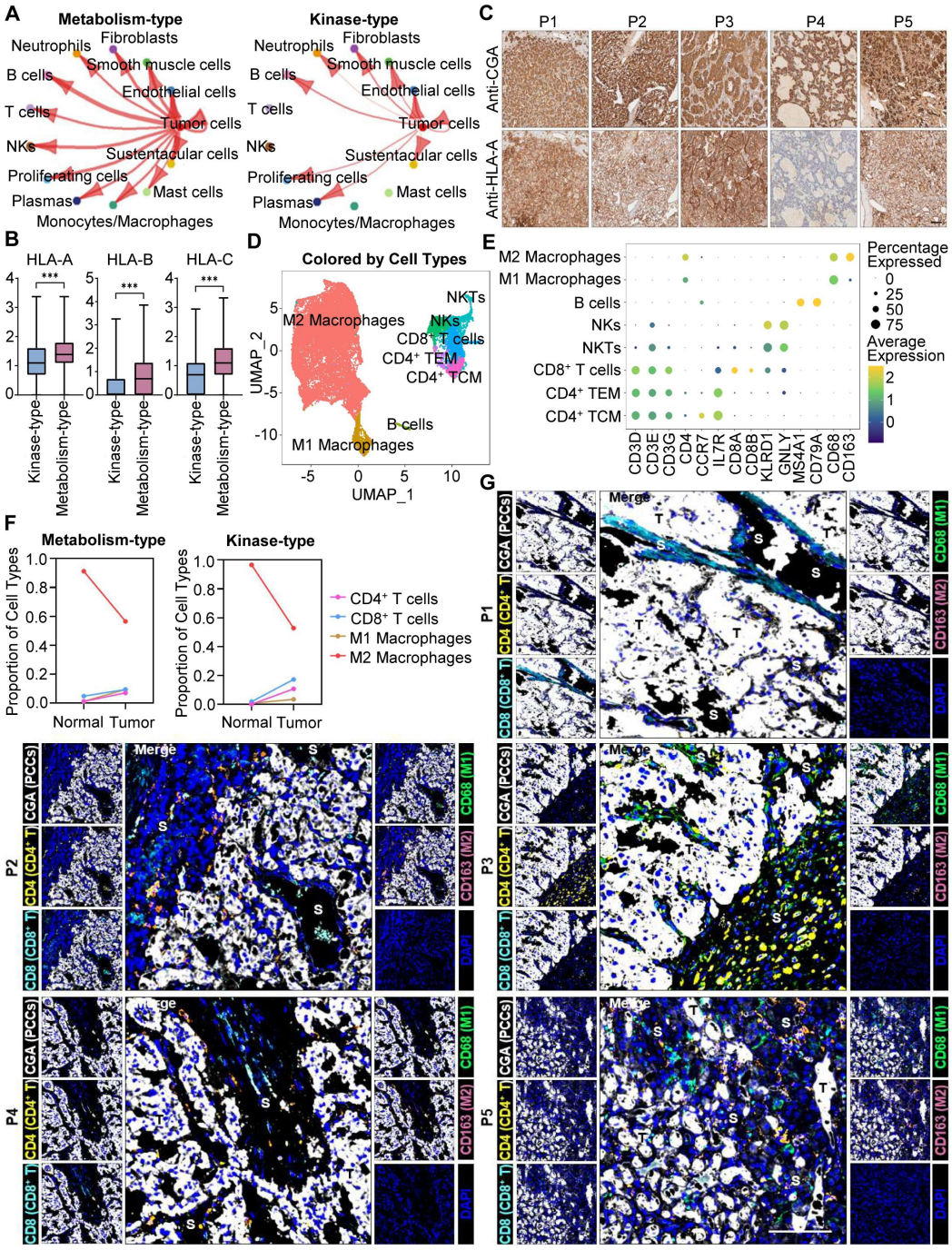

Figure 7.

Prediction of the Immune Escape Potential and Immunotherapy Response of PCC Patients.

(A) Circle plots depicting inferred cellular interactions in metabolism-type (left) and kinase-type (right) PCC microenvironment. (B) Box plots showing the expression levels of *HLA-A*, *HLA-B*, and *HLA-C* in metabolism-type and kinase-type PCC patients. (C) Immunohistochemistry staining of CGA and HLA-A in formalin-fixed paraffin-embedded PCC tissue sections matched to scRNA-seq specimens. Scale bar, 100 μm. (D) UMAP plot showing 8 immune cell types detected from all PCC specimens. (E) Dot plot of representative marker genes for each immune cell type. The color scale represents the average marker gene expression level; dot size represents the percentage of cells expressing a given marker gene. (F) Comparison of the proportion of immune cell types in tumor *vs* adjacent tissues. (G) Multispectral immunofluorescent staining for the juxtaposition of PCC cells (marked by CGA), $CD4^+$ T cells (marked by CD4), $CD8^+$ T cells (marked by CD8), M1 macrophages (marked by CD68), and M2 macrophages (marked by CD163) in formalin-fixed paraffin-embedded PCC tissue sections matched to scRNA-seq specimens. The white, yellow, cyan, green, pink, and blue spots indicated cells with high expression of CGA, CD4, CD8, CD68, CD163, and DAPI proteins in PCC tissue sections, respectively. S, stroma; T, tumor. Scale bar, 100 μm.

(Jhunjhunwala *et al*., 2021). As the scRNA-seq data do not support discernment of whether immune cells have infiltrated tumors or are merely present in the sampled materials, we performed multispectral immunofluorescence (mIF) staining on $CD4^+$ T cells, $CD8^+$ T cells, M1 macrophages, and M2 macrophages in formalin-fixed paraffin-embedded (FFPE) tumor tissues of P1-P5. We observed that $CD8^+$ T cells, as well as $CD4^+$ T cells, M1 macrophages, and M2 macrophages were rare (and were only present in tumor stroma of P1-P5), indicating apparent immune escape in both metabolism-type and kinase-type PCCs (**Fig. 7G**). Combined with previously reported negative regulatory effects of kinases (such as RET, ALK, and MEK) on HLA-I expression on tumor cells (Brea *et al*., 2016; Oh *et al*., 2019), we speculate that the possible reason for inability in recruiting $CD8^+$ T cells of kinase-type PCCs is the down-regulation of *HLA-I* in tumor cells regulated by *RET*, while the mechanism of immune escape in metabolism-type PCCs (with antigen presentation ability) needs to be further explored. Our results also indicate that the application of immunotherapy to metabolism-type PCCs is likely unsuitable, while kinase-type PCCs may have the potential of combined therapy with kinase inhibitors and immunotherapy.

Discussion

The genomic research of PCCs has made continuous progress in recent years (Bausch *et al*, 2017; Crona *et al*., 2017; Fishbein *et al*., 2017; Neumann *et al*, 2019), but there have been obvious breakthroughs for more efficacious therapies. Isotope therapies can only relieve the clinical symptoms in 50% of patients (without reducing tumor size) (Fitzgerald *et al*, 2006; Roman-Gonzalez & Jimenez, 2017), while most chemotherapies and targeted therapies exhibit low remission rates and severe side effects in clinical studies (Druce *et al*, 2009; Hamidi, 2019; O'Kane *et al*, 2019; Oh *et al*, 2012), limiting the development of PCC treatments. Although immunotherapy has achieved success in the therapy of solid tumors, it is difficult to evaluate the curative effect in PCCs. To address this problem, two key features associated with the tumor immunotherapy need to be elucidated—tumor heterogeneity and the tumor microenvironment (Hegde & Chen, 2020; Li *et al*, 2018; Zhang & Zhang, 2020). Regarding PCC heterogeneity, genomic studies have confirmed the inter-individual heterogeneity based on driver mutations (Dahia, 2014; Toledo *et al*., 2017). However, there is lack of relevant research on intra-tumoral heterogeneity, which has an impact on disease progression and sensitivity to immunotherapy (Vitale *et al*, 2021). For the PCC microenvironment, the cell composition and cellular crosstalk have not been explored. By investigating the heterogeneity and microenvironment characteristics of PCCs, we proposed a feasible method to judge the heterogeneity of PCCs, and also provided a clue for the application of immunotherapy in PCC patients.

The clinical and histopathological diagnosis of malignancy and heterogeneity of PCCs is particularly difficult, and is still limited by the lack of reliable prognostic markers (de Wailly *et al*., 2012). Although the PASS scoring system was proposed as a tool for discriminating potentially malignant PCCs from benign ones, it still cannot be reliably applied to PCCs for predicting malignancy or clinical prognostication, owing to observer variation and nonrepeatability (Agarwal *et al*., 2010; Kimura *et al*, 2014; Thompson, 2002; Wu *et al*., 2009). In order to investigate the association between PASS scoring system and heterogeneity of PCCs, we studied by scRNA-seq and observed less heterogeneity among different intra-tumoral sites than that among PCC patients, which is inconsistent with the prediction of the pathological PASS scoring system. Our findings suggest that the biopsy used to guide clinical treatment in the future may not need multi-point sampling, whereas and single-point sampling (while avoiding obvious necrotic areas) plus scRNA-seq analysis can informatively represent the characteristics of PCCs. Our findings also demonstrate that the PASS score is not suitable to reflect the intra-tumoral heterogeneity and inter-individual heterogeneity of PCCs, and helps explain the inconsistency between PASS score prediction and clinical outcomes in previous studies (Agarwal *et al*., 2010; Wu *et al*., 2009). Since the development of a reproducible modified scoring system for PCCs remains a challenging

task (Wu *et al*., 2009), the combination of molecular diagnostic methods like single-cell sequencing with pathological tools might be easier to implement in the clinical practice of PCC diagnosis and care (Crona *et al*., 2017; Papathomas *et al*, 2021).

According to the results of genomics research in recent years, 40~50% of PCCs have been classified into a certain molecular pathway (pseudohypoxia, kinase, or Wnt), but the remaining 50-60% are still unclassified (Crona *et al*., 2017; Lenders *et al*., 2014). PCCs that classified into these molecular pathways may have the opportunity to carry out drug clinical trials against corresponding targets, such as HIF2α, VEGF, and RET, etc. (Favier *et al*., 2015; Nölting *et al*, 2019; Toledo & Jimenez, 2018), while unclassified PCCs still have no clues or basis for drug treatment. According to the WES results of the 5 patients in our study, except for one patient with *VHL* germline mutation, the others could not be classified based on detected germline or somatic mutations. Therefore, we developed a new classification of PCCs based on scRNA-seq, which are able to accurately capture the transcriptional features of PCC cells. We found that PCC cells from 4 patients highly expressed metabolism-related genes, while that from another patient exhibited high expression of kinase-related genes. Although previous studies applying bulk RNA-seq analysis of PCCs have also reported highly expressed genes (Batchu *et al*, 2022; Flynn *et al*, 2015), the interpretation of bulk RNA-seq data can be complicated by interference from the large number of non-tumor cells (Potter, 2018; Suvà & Tirosh, 2019), so it is difficult to determine whether the highly expressed genes are reliable molecular features of PCCs. Although PCC cells from more patients need to be examined, we have defined at least two types of PCCs: metabolism-type and kinase-type.

One definition of the tumor immune microenvironment is the combination of the antigen presentation ability of tumor cells, the infiltration of immune cells, and the interaction between them (Joyce & Fearon, 2015; Schumacher & Schreiber, 2015). Although our immunofluorescence staining data showed a lack of $CD8^+$ T cell infiltration in both metabolism-type and kinase-type PCCs, only kinase-type PCCs exhibited downregulation of *HLA-I* molecules. The expression of HLA-I is a marker for tumor antigen presentation and $CD8^+$ T cell infiltration (Chowell *et al*, 2018; Jhunjhunwala *et al*., 2021; Perea *et al*, 2018). Previous studies have demonstrated that kinases such as RET, MAP2K1, ALK, and FGF can promote tumor growth via helping tumor cells to evade the immune system by downregulating HLA-I expression (Brea *et al*., 2016; Oh *et al*., 2019). The kinase-type PCCs that we defined exhibited activation of RET and FGF signals, which led us to consider the possible inhibitory effect of kinases on HLA-I expression in PCCs. Recently, RET inhibitors have been approved for the treatment of non-small cell lung cancer with *RET* mutation (Drilon *et al*, 2020). For kinase-type PCCs, whether RET inhibitors can enhance the antigen presentation ability of tumor cells, and further provide chance for combination of kinase-targeted therapy and immunotherapy, needs to be verified by follow-up research. The metabolism-type PCCs, however, with antigen presentation ability and also the lack of $CD8^+$ T cell infiltration, the application of immunotherapy is likely unsuitable, and the mechanism(s) of immune escape in these tumors needs to be further explored.

There are potential limitations of our study. Despite the patient cohort in our study including a hereditary PCC patient, only one patient with a *VHL* germline mutation was included; other types of hereditary PCCs with germline mutations (for example in *SDHx* and *FH*) were not included. The number of sporadic cases was also limited, mainly caused by the low incidence of PCCs. In addition, the specimens were all from primary tumors, while no metastatic tumors were included. Together, these considerations underscore the necessary for additional studies of PCCs in the future.

In summary, our study presents the molecular classification and tumor microenvironment characterization of PCCs through scRNA-seq. Our identification of less intra-tumoral heterogeneity than inter-individual heterogeneity of PCCs is inconsistent with the PASS score prediction and suggests the limitation of the PASS scoring system. Among unclassified PCCs, we defined

metabolism-type and kinase-type at the single-cell transcriptome level. We observed a lack of $CD8^+$ T cell infiltration in both metabolism-type and kinase-type PCCs. The kinase-type PCC showed downregulation of *HLA-I* that possibly regulated by *RET*, suggesting the potential of combined therapy with kinase inhibitors and immunotherapy in kinase-type PCCs. For the metabolism-type PCCs, which have antigen presentation ability and also exhibit immune escape, the application of immunotherapy is likely unsuitable. The proposal of this molecular classification and our characterization of these PCC types can contribute to strategy development and clinical trials of PCC treatments in the future.

Methods

Ethical Regulations

The research presented here complies with all relevant local, national, and international regulations. For all PCC patient specimens, informed written consent was obtained prior to donation. The Peking University First Hospital Review Board (Protocol 300-001) approved the study.

Patient Cohort

Five PCC patients were included, and all patients had signed the consent forms at the Department of Urology in Peking University First Hospital. Fresh tumor specimens were collected during surgical resection. The sporadic patients (P1-P4) were performed surgical resections of the tumors at right adrenals, and the VHL patient (P5) underwent left adrenalectomy. We collected 1 resected tumor specimen from P1 (P1_T1), 3 specimens from distinct intra-tumoral sites from P2 (P2_T1, P2_T2, and P2_T3) or P5 (P5_T1, P5_T2, and P5_T3), and 2 specimens from distinct intra-tumoral sites from P3 (P3_T1 and P3_T2), or P4 (P4_T1 and P4_T2). To enable comparisons, one adrenal tissue specimen adjacent to the tumor was collected from each patient (P1_A, P2_A, P3_A, P4_A, and P5_A). A total of sixteen specimens were carefully dissected under the microscope and confirmed by a qualified pathologist.

Tissue Processing

The fresh tumor specimens were stored in the tissue preservation solution (JSENB) and washed with Hanks Balanced Salt Solution (HBSS, HyClone) for 3 times and minced into 1-2 mm pieces. Then the tissue pieces were digested with 2 ml tissue dissociation solution at 37°C for 15 min in 15 ml centrifuge tube with sustained agitation. After digestion, using 40 μm sterile strainers to filter the samples and centrifuging the samples at 1,000 rpm for 5 min. Then the supernatant was discarded, and the sediment was resuspended in 1 ml phosphate buffered saline (PBS, HyClone). To remove the red blood cells, 2 ml red blood cell lysis buffer (BD) was added at 25°C for 10 min. The solution was then centrifuged at 500 g for 5 min and suspended in PBS. The cells were stained with trypan blue (Sigma) and microscopically evaluated.

Single-cell Library Construction and Sequencing

Utilizing the 10x Genomics Chromium Single Cell 3' v3 Library Kit and Chromium instrument, approximately 17,500 cells were partitioned into nanoliter droplets to achieve single-cell resolution for a maximum of 10,000 individual cells per sample. The resulting cDNA was tagged with a common 16 nt cell barcode and 10 nt Unique Molecular Identifier during the RT reaction. Full-length cDNA from poly-A mRNA transcripts was enzymatically fragmented and size selected to optimize the cDNA amplicon size (approximately 400 bp) for library construction (10x Genomics). The concentration of the 10x single-cell library was accurately determined through qPCR (Kapa Biosystems) to produce cluster counts appropriate for the HiSeq4000 or NovaSeq6000

platform (Illumina). In all, 26 × 98 bp (3' v3 libraries) sequence data were generated targeting between 25 and 50K read pairs/cell, which provided digital gene expression profiles for each individual cell.

General scRNA-seq Data Analysis

For single-cell RNA-seq analysis, we used CellRanger (10x Genomics, v.6.1.2) to pre-process the single-cell RNA-seq data after obtaining the paired-end raw reads. Cell barcodes and unique molecular identifiers (UMIs) of the library were extracted from read 1. Then, the reads were split according to their cell (barcode) IDs, and the UMI sequences from read 2 were simultaneously recorded for each cell. Quality control on these raw readings was subsequently performed to eliminate adapter contamination, duplicates, and low-quality bases. After filtering barcodes and low-quality readings that were not related to cells, we mapped the cleaned readings to the human genome (GRCh38) and retained the uniquely mapped readings for UMIs counts. Next, we estimated the accurate molecular counts and generated a UMI count matrix for each cell by counting UMIs for each sample. Finally, we generated a gene-barcode matrix that showed the barcoded cells and gene expression counts.

The R package Seurat (v.4.0.2) was used for all subsequent analysis (Butler *et al*., 2018; Satija *et al*., 2015; Stuart *et al*., 2019). For quality control of single-cell RNA-seq, a series of quality filters was applied to the data to remove those barcodes which fell into any one of these categories: too few genes expressed (possible debris), too many UMIs associated (possible more than one cell), and too high mitochondrial gene expression (possible dead cell). The cutoffs for these filters were as recommended by the Seurat package. Low-quality cells and outliers were discarded, and the single cells that passed the QC criteria were used for downstream analyses.

Cell Clustering and Cell Type Annotation

The Seurat software package (v.4.0.2) was used to perform cell clustering analysis to identify major cell types (Butler *et al*., 2018; Satija *et al*., 2015; Stuart *et al*., 2019). All Seurat objects constructed from the filtered UMI-based gene expression matrixes of given samples were merged. We first applied the SCTransform (v.0.3.2) function to implement normalization, variance stabilization, and feature selection through a regularized negative binomial model. Then, the principal component analysis (PCA) was applied for linear dimensionality reduction with the top 3000 variable genes. According to standard steps implemented in Seurat, highly variable numbers of principal components (PCs) 1-50 were selected and used for clustering using the Uniform Manifold Approximation and Projection (UMAP) method. We identified cell types of these clusters based on the expression of canonic cell type markers or inferred by CellMarker database (Zhang *et al*, 2019). The cluster markers were also certified using the FindAllMarkers function of the Seurat suite, and cell types were manually annotated based on certified markers finally.

Correlation Analysis of scRNA-seq

After integration, for each cluster, each sample, and each patient, we compared the gene expression to others to identify the significant highly expressed genes (adjusted P-value < 0.05 and log fold change > 0). Then the average gene expressions in each cluster, each sample, and each patient were calculated. The pairwise correlations were then estimated.

DEGs Identification and Enrichment Analysis

The cluster-specific genes were identified by running Seurat containing the function of FindAllMarkers on a log-transformed expression matrix (min. pct = 0. 25, only. Pos = TRUE, and logfc.threshold = 0.25). We also identified the differentially over-expressed genes between two clusters with the Wilcoxon Rank-Sum Test with the FindMarkers function in Seurat (adjusted P-value < 0.05, only.pos = T, and logfc.threshold = 0.1), and the cluster-specific overrepresented GO biological process was calculated with the compareCluster function in the clusterProfiler package

(v.4.2.2) of R (Yu *et al*, 2012). We also used the GSEA with the curated gene sets to identify the pathways that were induced or repressed in between the cell clusters. In brief, the mean gene expression level was calculated and the log twofold change (FC) between the specific cell cluster and the other cells was applied as the test statistic. The 50 hallmark gene sets in the MSigDB databases (*https://www.gsea-msigdb.org/gsea/msigdb*) were used for the GSEA analysis (Liberzon *et al*., 2011).

Single-cell RNA CNV Detection and Clustering

All cells were classified as either normal or tumor based on the genome-wide copy number profiles computed from the gene expression UMI matrix using the Bayesian segmentation approach, CopyKat (v.1.0.8) (Gao *et al*., 2021). Aneuploid single cells with genome-wide copy number aberrations were predicted to be tumor cells. Diploid cells were predicted to be normal cells. The CopyKat-based predictions were further confirmed by single-cell gene expression profiles.

Trajectory Analysis of scRNA-Seq Data

In order to perform a detailed comparison among different trajectory modeling tools, the Dynverse (v.0.1.2) tool was used (Saelens *et al*., 2019). Based on the scoring system provided by Dynverse and following a careful inspection of the generated trajectories, we applied 'SCORPIUS' and 'EMBEDDR' to infer the development trajectories. Finally, we selected the genes that were differentially expressed on different stages through the trajectory and plotted the pseudotime heatmap.

Cellular Communication Analysis

Cell-cell interactions based on the expression of known ligand-receptor pairs in different cell types were inferred using CellChatDB (v.1.1.3) (Jin *et al*., 2021). In brief, we followed the official workflow and loaded the normalized counts into CellChat and applied the preprocessing functions 'identifyOverExpressedGenes', 'identifyOverExpressedInteractions', and 'projectData' with standard parameters set. As database we selected the 'Secreted Signaling' pathways and used the pre-compiled human 'Protein-Protein-Interactions' as a priori network information. For the main analyses the core functions 'computeCommunProb', 'computeCommunProbPathway', and 'aggregateNet' were applied using standard parameters and fixed randomization seeds. Finally, to determine the senders and receivers in the network, the function 'netAnalysis_signalingRole' was applied on the 'netP' data slot.

Whole Exome Sequencing and Analysis

Genomic DNA extracted from tumor tissues were sent for whole exome sequencing. The exomes were captured using the Agilent SureSelect Human All Exon V6 Kit and the enriched exome libraries were constructed and sequenced on the Illumina NovaSeq 6000 platform to generate WES data (150 bp paired-end reads, > 100×) according to standard manufacturer protocols. The cleaned reads were aligned to the human reference genome sequence UCSC Build 19 (hg19) using Burrows-Wheeler Aligner (BWA) (v.0.7.12) (Li & Durbin, 2009). All aligned BAM were then performed through the same bioinformatics pipeline according to GATK Best Practices (v.3.8) (McKenna *et al*, 2010). We obtained germline variants based on variant calling from GATK-HaplotypeCaller. We then used GATK-MuT ect2 to call somatic variants in tumors and obtained a high-confidence mutation set after rigorous filtering by GATK-FilterMutectCalls. All variants were annotated using ANNOVAR (v.2018Apr16) (Wang *et al*, 2010).

Immunocytochemistry and Multispectral Immunofluorescent Staining

Immunocytochemistry and multispectral immunofluorescent staining experiments were conducted according to standard protocols using antibodies against formalin-fixed paraffin-embedded (FFPE) tissue specimens. The antibodies used are listed as follows: CGA (ABclonal, A9576), NDUFA4L2 (Proteintech, 66050-1-lg), COX4I2 (Santa, sc-100522), PNMT (Abcam, ab154282), RET (Abcam, ab134100), CD4 (Abcam, ab133616), CD8 (Invitrogen, MA1-80231), CD68 (Invitrogen, MA5-12407), CD163 (Abcam, ab182422), and HLA-A (ABclonal, A11406).

Data availability

Fastq raw data and processed data can be requested by contacting the corresponding authors. Human transcriptome reference used for our analysis is available at 10x Genomics website (*https://cf.10xgenomics.com/supp/cell-exp/refdata-cellranger-GRCh38-3.0.0.tar.gz*) or in zenodo (*https://zenodo.org/record/4114854/files/refdata-cellranger-GRCh38-3.0.0.tar.gz?download=1*).

Code availability

The single-cell RNA sequencing data was processed using cellranger v.6.1.2 (*https://www.10xgenomics.com/*) and analyzed with the R package Seurat v.4.0.2 (*https://satijalab.org/seurat/*). Custom code that was created for scRNA-seq analysis can be requested by contacting the corresponding authors.

Acknowledgements

This work was supported by grant from Ministry of Science and Technology of China (No. 2021YFA1300603 to L.S.), grant (Z200020 to L.S.) from the Natural Science Foundation of Beijing, grant (81874158 to L.S.) from the National Natural Science Foundation of China, and grant (2022CX08 to Z.Z.) from National High Level Hospital Clinical Research Funding. We thank Dr. Jiaqian Wang (YuCe Biotech Co., Ltd) for provided technical support.

Author contributions

Z.Z., L.S., and K.G. conceived the idea and designed the study. Y.X. prepared samples for scRNA-seq. S.Q. performed scRNA-seq data analysis. Q.S., S.F., W.A., Y.X., and W.H. performed immunocytochemistry and multispectral immunofluorescent staining. S.Y., K.Z., and X.Z. provided technical assistance. Z.Z., L.S., and Y.W. provided guidance in data analysis and interpretation of the results. S.Q. drafted the manuscript, with significant input from Z.Z., L.S., and K.G. All authors reviewed the manuscript prior to submission.

CONFLICT of INTEREST STATEMENTS

The authors declare no conflicts of interest that pertain to this work.

References

1. Agarwal A, Mehrotra PK, Jain M, Gupta SK, Mishra A, Chand G, Agarwal G, Verma AK, Mishra SK, Singh U (2010) **Size of the tumor and pheochromocytoma of the adrenal gland scaled score (PASS): can they predict malignancy?** *World J Surg* **34**:3022–3028

2. Batchu S, Hakim A, Henry OS, Madzo J, Atabek U, Spitz FR, Hong YK (2022) **Transcriptome-guided resolution of tumor microenvironment interactions in pheochromocytoma and paraganglioma subtypes** *Journal of endocrinological investigation* **45**:989–998

3. Bausch B, Schiavi F, Ni Y, Welander J, Patocs A, Ngeow J, Wellner U, Malinoc A, Taschin E, Barbon G, et al (2017) **Clinical Characterization of the Pheochromocytoma and Paraganglioma Susceptibility Genes SDHA, TMEM127, MAX, and SDHAF2 for Gene-Informed Prevention** *JAMA oncology* **3**:1204–1212

4. Brahmer JR, Tykodi SS, Chow LQ, Hwu WJ, Topalian SL, Hwu P, Drake CG, Camacho LH, Kauh J, Odunsi K, et al (2012) **Safety and activity of anti-PD-L1 antibody in patients with advanced cancer** *The New England journal of medicine* **366**:2455–2465

5. Bratslavsky G, Necchi A, Shapiro O, Jacob J, Gay LM, Alexander BM, Elvin JA, Vergilio J-A, Killian JK, Nho NT, et al (2019) **Malignant pheochromocytoma: A comprehensive genomic profiling study** :508–508

6. Brea EJ, Oh CY, Manchado E, Budhu S, Gejman RS, Mo G, Mondello P, Han JE, Jarvis CA, Ulmert D, et al (2016) **Kinase Regulation of Human MHC Class I Molecule Expression on Cancer Cells** *Cancer Immunol Res* **4**:936–947

7. Butler A, Hoffman P, Smibert P, Papalexi E, Satija R (2018) **Integrating single-cell transcriptomic data across different conditions, technologies, and species** *Nat Biotechnol* **36**:411–420

8. Califano D, Monaco C, de Vita G, D'Alessio A, Dathan NA, Possenti R, Vecchio G, Fusco A, Santoro M, de Franciscis V (1995) **Activated RET/PTC oncogene elicits immediate early and delayed response genes in PC12 cells** *Oncogene* **11**:107–112

9. Chappell JC, Payne LB, Rathmell WK (2019) **Hypoxia, angiogenesis, and metabolism in the hereditary kidney cancers** *J Clin Invest* **129**:442–451

10. Chowell D, Morris LGT, Grigg CM, Weber JK, Samstein RM, Makarov V, Kuo F, Kendall SM, Requena D, Riaz N, et al (2018) **Patient HLA class I genotype influences cancer response to checkpoint blockade immunotherapy** *Science (New York, NY)* **359**:582–587

11. Crona J, Taïeb D, Pacak K (2017) **New Perspectives on Pheochromocytoma and Paraganglioma: Toward a Molecular Classification** *Endocr Rev* **38**:489–515

12. Dahia PL (2014) **Pheochromocytoma and paraganglioma pathogenesis: learning from genetic heterogeneity** *Nature reviews Cancer* **14**:108–119

13. Dai C, Liang S, Sun B, Kang J (2020) **The Progress of Immunotherapy in Refractory Pituitary Adenomas and Pituitary Carcinomas** *Front Endocrinol (Lausanne* **11**

14. de Wailly P, Oragano L, Radé F, Beaulieu A, Arnault V, Levillain P, Kraimps JL (2012) **Malignant pheochromocytoma: new malignancy criteria** *Langenbecks Arch Surg* **397**:239–246

15. Drilon A, Hu ZI, Lai GGY, Tan DSW (2018) **Targeting RET-driven cancers: lessons from evolving preclinical and clinical landscapes** *Nature reviews Clinical oncology* **15**:151–167

16. Drilon A, Oxnard GR, Tan DSW, Loong HHF, Johnson M, Gainor J, McCoach CE, Gautschi O, Besse B, Cho BC, et al (2020) **Efficacy of Selpercatinib in RET Fusion-Positive Non-Small-Cell Lung Cancer** *The New England journal of medicine* **383**:813–824

17. Druce MR, Kaltsas GA, Fraenkel M, Gross DJ, Grossman AB (2009) **Novel and evolving therapies in the treatment of malignant phaeochromocytoma: experience with the mTOR inhibitor everolimus (RAD001)** *Hormone and metabolic research = Hormon-und Stoffwechselforschung = Hormones et metabolisme* **41**:697–702

18. Favier J, Amar L, Gimenez-Roqueplo AP (2015) **Paraganglioma and phaeochromocytoma: from genetics to personalized medicine** *Nature reviews Endocrinology* **11**:101–111

19. Fishbein L, Leshchiner I, Walter V, Danilova L, Robertson AG, Johnson AR, Lichtenberg TM, Murray BA, Ghayee HK, Else T, et al (2017) **Comprehensive Molecular Characterization of Pheochromocytoma and Paraganglioma** *Cancer Cell* **31**:181–193

20. Fitzgerald PA, Goldsby RE, Huberty JP, Price DC, Hawkins RA, Veatch JJ, Dela Cruz F, Jahan TM, Linker CA, Damon L, et al (2006) **Malignant pheochromocytomas and paragangliomas: a phase II study of therapy with high-dose 131I-metaiodobenzylguanidine (131I-MIBG)** *Annals of the New York Academy of Sciences* **1073**:465–490

21. Flynn A, Benn D, Clifton-Bligh R, Robinson B, Trainer AH, James P, Hogg A, Waldeck K, George J, Li J, et al (2015) **The genomic landscape of phaeochromocytoma** *The Journal of pathology* **236**:78–89

22. Gao R, Bai S, Henderson YC, Lin Y, Schalck A, Yan Y, Kumar T, Hu M, Sei E, Davis A, et al (2021) **Delineating copy number and clonal substructure in human tumors from single-cell transcriptomes** *Nat Biotechnol* **39**:599–608

23. Gastardelo TS, Cunha BR, Raposo LS, Maniglia JV, Cury PM, Lisoni FC, Tajara EH, Oliani SM (2014) **Inflammation and cancer: role of annexin A1 and FPR2/ALX in proliferation and metastasis in human laryngeal squamous cell carcinoma** *PLoS One* **9**

24. Gavins FN, Yona S, Kamal AM, Flower RJ, Perretti M (2003) **Leukocyte antiadhesive actions of annexin 1: ALXR-and FPR-related anti-inflammatory mechanisms** *Blood* **101**:4140–4147

25. Gerke V, Moss SE (2002) **Annexins: from structure to function** *Physiol Rev* **82**:331–371

26. Guo D, Zhao X, Wang A, Xie Q, Xu X, Sun J (2019) **PD-L1 expression and association with malignant behavior in pheochromocytomas/paragangliomas** *Human pathology* **86**:155–162

27. Hamidi O (2019) **Metastatic pheochromocytoma and paraganglioma: recent advances in prognosis and management** *Current opinion in endocrinology, diabetes, and obesity* **26**:146–154

28. Hayhoe RP, Kamal AM, Solito E, Flower RJ, Cooper D, Perretti M (2006) **Annexin 1 and its bioactive peptide inhibit neutrophil-endothelium interactions under flow: indication of distinct receptor involvement** *Blood* **107**:2123–2130

29. Hegde PS, Chen DS (2020) **Top 10 Challenges in Cancer Immunotherapy** *Immunity* **52**:17–35

30. Herbst RS, Soria JC, Kowanetz M, Fine GD, Hamid O, Gordon MS, Sosman JA, McDermott DF, Powderly JD, Gettinger SN, et al (2014) **Predictive correlates of response to the anti-PD-L1 antibody MPDL3280A in cancer patients** *Nature* **515**:563–567

31. Jhunjhunwala S, Hammer C, Delamarre L (2021) **Antigen presentation in cancer: insights into tumour immunogenicity and immune evasion** *Nature reviews Cancer* **21**:298–312

32. Jin S, Guerrero-Juarez CF, Zhang L, Chang I, Ramos R, Kuan CH, Myung P, Plikus MV, Nie Q (2021) **Inference and analysis of cell-cell communication using CellChat** *Nat Commun* **12**

33. Joyce JA, Fearon DT (2015) **T cell exclusion, immune privilege, and the tumor microenvironment** *Science (New York, NY)* **348**:74–80

34. Katoh M (2016) **Therapeutics Targeting FGF Signaling Network in Human Diseases** *Trends in pharmacological sciences* **37**:1081–1096

35. Kimura N, Takayanagi R, Takizawa N, Itagaki E, Katabami T, Kakoi N, Rakugi H, Ikeda Y, Tanabe A, Nigawara T, et al (2014) **Pathological grading for predicting metastasis in phaeochromocytoma and paraganglioma** *Endocrine-related cancer* **21**:405–414

36. Kubota-Nakayama F, Nakamura Y, Konosu-Fukaya S, Azmahani A, Ise K, Yamazaki Y, Kitawaki Y, Felizola SJ, Ono Y, Omata K, et al (2016) **Expression of steroidogenic enzymes and their transcription factors in cortisol-producing adrenocortical adenomas: immunohistochemical analysis and quantitative real-time polymerase chain reaction studies** *Human pathology* **54**:165–173

37. Kulkarni MM, Khandeparkar SG, Deshmukh SD, Karekar RR, Gaopande VL, Joshi AR, Kesari MV, Shelke RR (2016) **Risk Stratification in Paragangliomas with PASS (Pheochromocytoma of the Adrenal Gland Scaled Score) and Immunohistochemical Markers** *Journal of clinical and diagnostic research : JCDR* **10**:Ec01–ec04

38. Lam AK (2017) **Update on Adrenal Tumours in 2017 World Health Organization (WHO) of Endocrine Tumours** *Endocrine pathology* **28**:213–227

39. Lenders JW, Duh QY, Eisenhofer G, Gimenez-Roqueplo AP, Grebe SK, Murad MH, Naruse M, Pacak K, Young WF (2014) **Pheochromocytoma and paraganglioma: an endocrine society clinical practice guideline** *J Clin Endocrinol Metab* **99**:1915–1942

40. Lewis PD (1971) **A cytophotometric study of benign and malignant phaeochromocytomas** *Virchows Arch B Cell Pathol* **9**:371–376

41. Li H, Durbin R (2009) **Fast and accurate short read alignment with Burrows-Wheeler transform** *Bioinformatics (Oxford, England)* **25**:1754–1760

42. Li J, Byrne KT, Yan F, Yamazoe T, Chen Z, Baslan T, Richman LP, Lin JH, Sun YH, Rech AJ, et al (2018) **Tumor Cell-Intrinsic Factors Underlie Heterogeneity of Immune Cell Infiltration and Response to Immunotherapy** *Immunity* **49**:178–193

43. Liang G, Liu Z, Wu J, Cai Y, Li X (2012) **Anticancer molecules targeting fibroblast growth factor receptors** *Trends in pharmacological sciences* **33**:531–541

44. Liberzon A, Subramanian A, Pinchback R, Thorvaldsdóttir H, Tamayo P, Mesirov JP (2011) **Molecular signatures database (MSigDB) 3.0** *Bioinformatics (Oxford, England)* **27**:1739–1740

45. Mahmoodi N, Harijan RK, Schramm VL (2020) **Transition-State Analogues of Phenylethanolamine N-Methyltransferase** *Journal of the American Chemical Society* **142**:14222–14233

46. McKenna A, Hanna M, Banks E, Sivachenko A, Cibulskis K, Kernytsky A, Garimella K, Altshuler D, Gabriel S, Daly M, et al (2010) **The Genome Analysis Toolkit: a MapReduce framework for analyzing next-generation DNA sequencing data** *Genome research* **20**:1297–1303

47. Naing A, Meric-Bernstam F, Stephen B, Karp DD, Hajjar J, Rodon Ahnert J, Piha-Paul SA, Colen RR, Jimenez C, Raghav KP, et al (2020) **Phase 2 study of pembrolizumab in patients with advanced rare cancers** *Journal for immunotherapy of cancer*

48. Neumann HPH, Young WF, Eng C (2019) **Pheochromocytoma and Paraganglioma** *The New England journal of medicine* **381**:552–565

49. Nölting S, Grossman A, Pacak K (2019) **Metastatic Phaeochromocytoma: Spinning Towards More Promising Treatment Options. Experimental and clinical endocrinology & diabetes : official journal** *German Society of Endocrinology [and] German Diabetes Association* **127**:117–128

50. O'Kane GM, Ezzat S, Joshua AM, Bourdeau I, Leibowitz-Amit R, Olney HJ, Krzyzanowska M, Reuther D, Chin S, Wang L, et al (2019) **A phase 2 trial of sunitinib in patients with progressive paraganglioma or pheochromocytoma: the SNIPP trial** *British journal of cancer* **120**:1113–1119

51. Oh CY, Klatt MG, Bourne C, Dao T, Dacek MM, Brea EJ, Mun SS, Chang AY, Korontsvit T, Scheinberg DA (2019) **ALK and RET Inhibitors Promote HLA Class I Antigen Presentation and Unmask New Antigens within the Tumor Immunopeptidome** *Cancer Immunol Res* **7**:1984–1997

52. Oh DY, Kim TW, Park YS, Shin SJ, Shin SH, Song EK, Lee HJ, Lee KW, Bang YJ (2012) **Phase 2 study of everolimus monotherapy in patients with nonfunctioning neuroendocrine tumors or pheochromocytomas/paragangliomas** *Cancer* **118**:6162–6170

53. Papathomas TG, Suurd DPD, Pacak K, Tischler AS, Vriens MR, Lam AK, de Krijger RR (2021) **What Have We Learned from Molecular Biology of Paragangliomas and Pheochromocytomas?** *Endocrine pathology* **32**:134–153

54. Perea F, Sánchez-Palencia A, Gómez-Morales M, Bernal M, Concha Á, García MM, González-Ramírez AR, Kerick M, Martin J, Garrido F, et al (2018) **HLA class I loss and PD-L1 expression in lung cancer: impact on T-cell infiltration and immune escape** *Oncotarget* **9**:4120–4133

55. Pillai S, Gopalan V, Lam AK (2017) **Review of sequencing platforms and their applications in phaeochromocytoma and paragangliomas** *Crit Rev Oncol Hematol* **116**:58–67

56. Pinato DJ, Black JR, Trousil S, Dina RE, Trivedi P, Mauri FA, Sharma R (2017) **Programmed cell death ligands expression in phaeochromocytomas and paragangliomas: Relationship with the hypoxic response, immune evasion and malignant behavior** *Oncoimmunology* **6**

57. Potter SS (2018) **Single-cell RNA sequencing for the study of development, physiology and disease** *Nature reviews Nephrology* **14**:479–492

58. Powers JF, Brachold JM, Tischler AS (2003) **Ret protein expression in adrenal medullary hyperplasia and pheochromocytoma** *Endocrine pathology* **14**:351–361

59. Powers JF, Picard KL, Tischler AS (2009) **RET expression and neuron-like differentiation of pheochromocytoma and normal chromaffin cells** *Hormone and metabolic research = Hormon- und Stoffwechselforschung = Hormones et metabolisme* **41**:710–714

60. Ribas A, Wolchok JD (2018) **Cancer immunotherapy using checkpoint blockade** *Science (New York, NY)* **359**:1350–1355

61. Roman-Gonzalez A, Jimenez C (2017) **Malignant pheochromocytoma-paraganglioma: pathogenesis, TNM staging, and current clinical trials** *Current opinion in endocrinology, diabetes, and obesity* **24**:174–183

62. Sade-Feldman M, Yizhak K, Bjorgaard SL, Ray JP, de Boer CG, Jenkins RW, Lieb DJ, Chen JH, Frederick DT, Barzily-Rokni M, et al (2018) **Defining T Cell States Associated with Response to Checkpoint Immunotherapy in Melanoma** *Cell* **175**:998–1013

63. Saelens W, Cannoodt R, Todorov H, Saeys Y (2019) **A comparison of single-cell trajectory inference methods** *Nat Biotechnol* **37**:547–554

64. Satija R, Farrell JA, Gennert D, Schier AF, Regev A (2015) **Spatial reconstruction of single-cell gene expression data** *Nat Biotechnol* **33**:495–502

65. Schumacher TN, Schreiber RD (2015) **Neoantigens in cancer immunotherapy** *Science (New York, NY)* **348**:69–74

66. Sherwin RP (1959) **Histopathology of pheochromocytoma** *Cancer* **12**:861–877

67. Sinkler CA, Kalpage H, Shay J, Lee I, Malek MH, Grossman LI, Hüttemann M (2017) **Tissue- and Condition-Specific Isoforms of Mammalian Cytochrome c Oxidase Subunits: From Function to Human Disease** *Oxidative medicine and cellular longevity* **2017**

68. Sisson JC, Shapiro B, Beierwaltes WH, Glowniak JV, Nakajo M, Mangner TJ, Carey JE, Swanson DP, Copp JE, Satterlee WG, et al (1984) **Radiopharmaceutical treatment of malignant pheochromocytoma** *J Nucl Med* **25**:197–206

69. Stanton SE, Disis ML (2016) **Clinical significance of tumor-infiltrating lymphocytes in breast cancer** *Journal for immunotherapy of cancer* **4**

70. Strong VE, Kennedy T, Al-Ahmadie H, Tang L, Coleman J, Fong Y, Brennan M, Ghossein RA (2008) **Prognostic indicators of malignancy in adrenal pheochromocytomas: clinical, histopathologic, and cell cycle/apoptosis gene expression analysis** *Surgery* **143**:759–768

71. Stuart T, Butler A, Hoffman P, Hafemeister C, Papalexi E, Mauck WM, Hao Y, Stoeckius M, Smibert P, Satija R (2019) **Comprehensive Integration of Single-Cell Data** *Cell* **177**:1888–1902

72. Suvà ML, Tirosh I (2019) **Single-Cell RNA Sequencing in Cancer: Lessons Learned and Emerging Challenges** *Molecular cell* **75**:7–12

73. Symington T, Goodall AL (1953) **Studies in phaeochromocytoma** *I. Pathological aspects. Glasgow Med J* **34**:75–96

74. Thompson LD (2002) **Pheochromocytoma of the Adrenal gland Scaled Score (PASS) to separate benign from malignant neoplasms: a clinicopathologic and immunophenotypic study of 100 cases** *The American journal of surgical pathology* **26**:551–566

75. Toledo R, Jimenez C (2018) **Recent advances in the management of malignant pheochromocytoma and paraganglioma: focus on tyrosine kinase and hypoxia-inducible factor inhibitors** *F1000Research*

76. Toledo RA, Burnichon N, Cascon A, Benn DE, Bayley JP, Welander J, Tops CM, Firth H, Dwight T, Ercolino T, et al (2017) **Consensus Statement on next-generation-sequencing-based diagnostic testing of hereditary phaeochromocytomas and paragangliomas** *Nature reviews Endocrinology* **13**:233–247

77. Uher O, Huynh TT, Zhu B, Horn LA, Caisova V, Hadrava Vanova K, Medina R, Wang H, Palena C, Chmelar J, et al (2021) **Identification of Immune Cell Infiltration in Murine Pheochromocytoma during Combined Mannan-BAM, TLR Ligand, and Anti-CD40 Antibody-Based Immunotherapy** *Cancers*

78. Vitale I, Shema E, Loi S, Galluzzi L (2021) **Intratumoral heterogeneity in cancer progression and response to immunotherapy** *Nature medicine* **27**:212–224

79. Vortmeyer AO, Falke EA, Gläsker S, Li J, Oldfield EH (2013) **Nervous system involvement in von Hippel-Lindau disease: pathology and mechanisms** *Acta Neuropathol* **125**:333–350

80. Wang K, Li M, Hakonarson H (2010) **ANNOVAR: functional annotation of genetic variants from high-throughput sequencing data** *Nucleic acids research* **38**

81. Wiedenmann B, Waldherr R, Buhr H, Hille A, Rosa P, Huttner WB (1988) **Identification of gastroenteropancreatic neuroendocrine cells in normal and neoplastic human tissue with antibodies against synaptophysin, chromogranin A, secretogranin I (chromogranin B), and secretogranin II** *Gastroenterology* **95**:1364–1374

82. Winkler H, Fischer-Colbrie R (1992) **The chromogranins A and B: the first 25 years and future perspectives** *Neuroscience* **49**:497–528

83. Wu D, Tischler AS, Lloyd RV, DeLellis RA, de Krijger R, van Nederveen F, Nosé V (2009) **Observer variation in the application of the Pheochromocytoma of the Adrenal Gland Scaled Score** *The American journal of surgical pathology* **33**:599–608

84. Yates R, Katugampola H, Cavlan D, Cogger K, Meimaridou E, Hughes C, Metherell L, Guasti L, King P (2013) **Adrenocortical development, maintenance, and disease** *Current topics in developmental biology* **106**:239–312

85. Yu G, Wang LG, Han Y, He QY (2012) **clusterProfiler: an R package for comparing biological themes among gene clusters** *Omics* **16**:284–287

86. Zhang X, Lan Y, Xu J, Quan F, Zhao E, Deng C, Luo T, Xu L, Liao G, Yan M, et al (2019) **CellMarker: a manually curated resource of cell markers in human and mouse** *Nucleic acids research* **47**:D721–d728

87. Zhang Y, Zhang Z (2020) **The history and advances in cancer immunotherapy: understanding the characteristics of tumor-infiltrating immune cells and their therapeutic implications** *Cellular & molecular immunology* **17**:807–821

Author information

Sen Qin
Department of Biochemistry and Molecular Biology, School of Basic Medical Sciences, Department of Urology, Peking University First Hospital, Peking University Health Science Center, Beijing 100191, China

Yawei Xu
Department of Biochemistry and Molecular Biology, School of Basic Medical Sciences, Department of Urology, Peking University First Hospital, Peking University Health Science Center, Beijing 100191, China

Shimiao Yu
Department of Biochemistry and Molecular Biology, School of Basic Medical Sciences, Department of Urology, Peking University First Hospital, Peking University Health Science Center, Beijing 100191, China

Wencong Han
Department of Biochemistry and Molecular Biology, School of Basic Medical Sciences, Department of Urology, Peking University First Hospital, Peking University Health Science Center, Beijing 100191, China

Shiheng Fan
Shenzhen Institute of Ladder for Cancer Research, Shenzhen 518020, China

Wenxiang Ai
Shenzhen Institute of Ladder for Cancer Research, Shenzhen 518020, China

Kenan Zhang
Department of Biochemistry and Molecular Biology, School of Basic Medical Sciences, Department of Urology, Peking University First Hospital, Peking University Health Science Center, Beijing 100191, China

Yizhou Wang
Department of Biochemistry and Molecular Biology, School of Basic Medical Sciences, Department of Urology, Peking University First Hospital, Peking University Health Science Center, Beijing 100191, China

Xuehong Zhou
Department of Biochemistry and Molecular Biology, School of Basic Medical Sciences, Department of Urology, Peking University First Hospital, Peking University Health Science Center, Beijing 100191, China

Qi Shen
Department of Biochemistry and Molecular Biology, School of Basic Medical Sciences, Department of Urology, Peking University First Hospital, Peking University Health Science Center, Beijing 100191, China

Kan Gong
Department of Biochemistry and Molecular Biology, School of Basic Medical Sciences, Department of Urology, Peking University First Hospital, Peking University Health Science Center, Beijing 100191, China
For correspondence:gongkan_pku@126.com

Luyang Sun
Department of Biochemistry and Molecular Biology, School of Basic Medical Sciences, Department of Urology, Peking University First Hospital, Peking University Health Science Center, Beijing 100191, China
For correspondence: luyang_sun@hsc.pku.edu.cn
ORCID iD: 0000-0003-3917-473X

Zheng Zhang
Department of Biochemistry and Molecular Biology, School of Basic Medical Sciences, Department of Urology, Peking University First Hospital, Peking University Health Science Center, Beijing 100191, China
For correspondence: doczhz@aliyun.com

Editors

Reviewing Editor
Yongliang Yang
Dalian University of Technology, China

Senior Editor
Caigang Liu
Shengjing Hospital of China Medical University, China

Reviewer #1 (Public Review):

Proposed significance: Targeted therapy in general has miraculous results.
Good and detailed study of molecular characteristics and microenvironment of tumor of PCCs .However molecular classification system based on limited number of cases is not acceptable.
Early diagnosis is of utmost importance in patient care and the next important is classification of tumor for treatment purposes.
Further research is needed to develop Molecular signature of tumor types . This will help in targeted therapy and precision medicine.

Strength: Molecular characterisation of tumor

Weakness: The sample size is very small from a statistical point of view to derive a conclusion. Only Observations can be recorded
Transcriptome profiles of 11 tumor tissues were studied but they belong to the same 5 patients.

Validation of tumor tissue: comparison is made with adjacent normal tissue (n=5)
Chromogranin IHC marker is used for identifying tumor cells. However, chromogranin marker positivity is also seen in normal adrenal medulla /chromaffin cells.
Any better evidence of Validation of tumor tissue?

Tumor microenvironment:
CD8+T cells: it is mentioned in the article that there is lack of CD8+ Tcells in both types of PCC,

(Page 5, line 16)

However Figures 7 D, E and F show presence of CD8+T cells. Needs clarification or quantification.

Tumor heterogeneity : Page 7 Line 5
PASS system is used by authors for predicting malignant potential and tumor heterogeneity. Molecular methods need to be used for evaluating tumor heterogeneity rather than histomorphology.

Ground of comparision is not valid. PASS system is based on histomorphology and present study/attempt at classification is based on molecular studies. So they cannot be compared .

Page 5 ,Line 18: HLA downregulation is observation and its regulation by RET is a possibility. Its involvement in tumor progression needs solid proof. So targeting kinase pathway for therapy is only a possibility.

Reviewer #2 (Public Review):

Pheochromocytoma (PCC), a rare neuroendocrine tumor, is currently considered malignant, but non-surgical treatment options are very limited and there is an urgent need for more basic research to support the development of new therapeutic approaches. In the present work, the authors described the intra- and inter-tumor heterogeneity by performing scRNA-seq on tumor samples from five patients with PCC, and evaluated the corresponding PASS scores.

Strengths: The tumor microenvironment of PCC was characterized and potential molecular classification criteria based on single-cell transcriptomics were proposed, offering new theoretical possibilities for the treatment of PCC. The article is logically written and the results are clearly presented.

Weaknesses: I still have concerns about some of the article's content. My main concerns are: In this study, the authors seem to have demonstrated the inaccuracy of a subjective score (PASS) by another objective means (scRNA-seq). In fact, the multiparametric scoring systems such as PASS are no longer endorsed in the 2022 WHO guidelines. The PASS scoring system does not have a high positive predictive value for risk stratification of PCC metastasis, but "rule-out" of metastasis risk with a PASS score of <4 seems to be fairly reliable. Could the authors please explain why the PASS scores were chosen rather than the GAPP, m-GAPP, or COPPS scoring systems? If possible, please try to emphasize the importance and necessity of using the PASS scoring system, either by replacing it with a more acceptable scoring system or by deleting the relevant part, which does not seem to be very relevant to the subject of the article.

Moreover, I noted the following statement in the text "There are no studies reporting the composition of immune cells in PCCs. The few published studies investigating the immune microenvironment of PCCs have been limited to the expression of PDL1 at the histological level and to assessment of the tumor mutation burden (TMB) at the genomic level, and these results only seem to suggest that PCCs are immune-cold (Bratslavsky et al, 2019; Guo et al, 2019; Pinato et al, 2017)." This statement is very wrong. The reason for this error may be that the authors did not adequately search and read the relevant literature. I noticed that almost all references in this paper are dated 2021 and earlier, which is surprising. Please update the references cited in this paper in a comprehensive and detailed manner; referring to literature published too early may lead to inadequate discussion or even one-sided or incorrect conclusions and conjectures.

For example, the text statement "Combined with previously reported negative regulatory effects of kinases (such as RET, ALK, and MEK) on HLA-I expression on tumor cells (Brea et

al., 2016; Oh et al., 2019), we speculate that the possible reason for inability in recruiting CD8+ T cells of kinase-type PCCs is the downregulation of HLA-I in tumor cells regulated by RET, while the mechanism of immune escape in metabolism-type PCCs (with antigen presentation ability) needs to be further explored. Our results also indicate that the application of immunotherapy to metabolism-type PCCs is likely unsuitable, while kinase-type PCCs may have the potential of combined therapy with kinase inhibitors and immunotherapy." is rather one-sided; in fact, the presence of immune escape in PCC, as the malignancy with the lowest tumor mutation compliance, has been well characterized, and the low number of infiltrating T cells in tumor tissue may be influenced by a variety of factors, such as the release of catecholamines, the expression of inhibitory receptors on the surface of T cells, and so on, although genetic mutation still plays the most crucial role. The Discussion section also has a lot of information that needs to be updated or corrected and expanded, so please rewrite the above section with sufficiently updated references.

Below I have listed some references for the authors to read:
Tufton N, Hearnden RJ, Berney DM, et al. The immune cell infiltrate in the tumour microenvironment of phaeochromocytomas and paragangliomas. Endocr Relat Cancer. 2022;29(11):589-598. Published 2022 Sep 19. doi:10.1530/ERC-22-0020
Jin B, Han W, Guo J, et al. Initial characterization of immune microenvironment in pheochromocytoma and paraganglioma. Front Genet. 2022;13:1022131. Published 2022 Dec 7. doi:10.3389/fgene.2022.1022131
Celada L, Cubiella T, San-Juan-Guardado J, et al. Pseudohypoxia in paraganglioma and pheochromocytoma is associated with an immunosuppressive phenotype. J Pathol. 2023;259(1):103-114. doi:10.1002/path.6026
Calsina B, Piñeiro-Yáñez E, Martínez-Montes ÁM, et al. Genomic and immune landscape Of metastatic pheochromocytoma and paraganglioma. Nat Commun. 2023;14(1):1122. Published 2023 Feb 28. doi:10.1038/s41467-023-36769-6

Reviewer #3 (Public Review):

The main findings of this study are as follows: (1) The authors defined "metabolism-type" and "kinase-type" in unclassified sporadic PCC patients through the single-cell transcriptomics-based differentially expressed genes and functional enrichment analyses. (2) They identified the limitation of Pheochromocytoma of the Adrenal gland Scaled Score (PASS) system and suggested the combination of molecular diagnostic methods like scRNA-seq with pathological tools like PASS in aiding the clinical evaluation of PCCs. (3) Analysis of the PCC microenvironment revealed a lack of immune cell infiltration in both metabolism-type and kinase-type PCCs, while only the kinase-type PCC patient exhibited the low expression of HLA-I that potentially regulated by RET, providing clues for the combined therapy with kinase inhibitors and immunotherapy in kinase-type PCC patients.

The main strength of this manuscript is that it involves scRNA-seq analysis of an extremely rare tumor type-PCCs, which presents a single-cell transcriptomics-based molecular classification and microenvironment characterization of PCCs and further provides clues for potential therapeutic strategies to treat PCCs. The authors also validated the scRNA-seq analysis results (such as the expression levels of marker genes and the distribution of immune cells in the PCC microenvironment) with immunocytochemistry and multispectral immunofluorescent staining. In summary, the findings in this manuscript are quite interesting and significant, which will potentially be valuable for the molecular classification of PCCs.